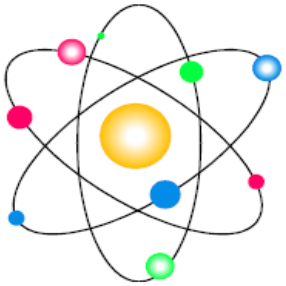

Nuclear Physics Across Energy Scales conference, C3NT, Wuhan

Alpha Clustering and Decay in Nuclei

Chang Xu

School of Physics, Nanjing University

Outline:

1. α cluster structure and motion
2. Cluster formation, dissolution and Pauli blockings
3. Quartetting wave function approach: ^{104}Te, ^{212}Po, ^{302}Lv

α cluster structure and motion

1. Single particle motion

The Nobel Prize in Physics 1963

Eugene Paul Wigner
Prize share: 1/2

Maria Goeppert Mayer
Prize share: 1/4

J. Hans D. Jensen
Prize share: 1/4

2. Collective motion

The Nobel Prize in Physics 1975

Aage Niels Bohr
Prize share: 1/3

Ben Roy Mottelson
Prize share: 1/3

Leo James Rainwater
Prize share: 1/3

3. Cluster motion

Light nuclei

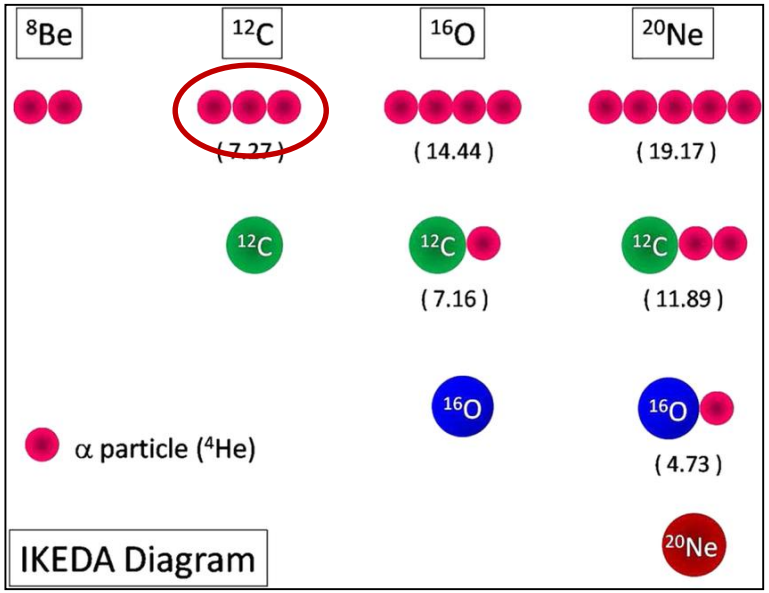

Heavy nuclei: α cluster decay

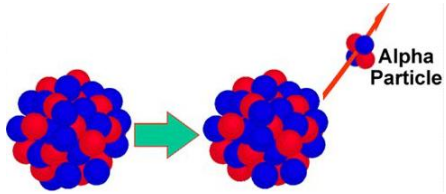

Chart of nuclides

Nuclei that exhibit α decay are indicated with a yellow background

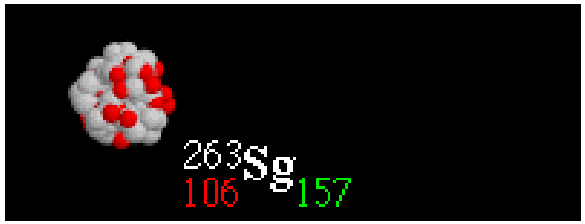

Z, number of protons

Doubly magic: ^{100}Sn

Superheavy island ^{298}Lv?

Doubly magic: ^{208}Pb

α decay typically occurs for heavy nuclei, Z larger than 50

Z=8
Z=20
Z=28
Z=50
Z=82
N=8
N=20
N=28
N=50
N=82
N=126

N, number of neutrons

Superheavy nuclei: α cluster decay chain

Will the periodic table ever be complete?

The periodic table currently consists of 118 elements, the last four of which were announced in 2016. The International Union of Pure and Applied Chemistry (IUPAC), which formally verifies, recognizes, and names new elements, has a challenging task. Its guidelines for the criteria for element discovery were established 29 years ago, yet in 2018, IUPAC issued an update illustrating the challenges associated with resolving whether the periodic table will ever be complete. IUPAC's updated report addressed how previously utilized methods and technologies for discovering new elements were being supplanted by innovative approaches. As new techniques are developed, it is possible more elements will be found–the limitations of human inventiveness may be our only obstacle.

Fusion reactions

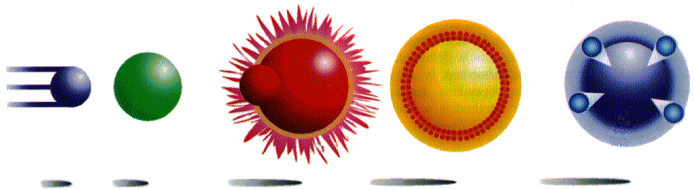

α cluster decay chain

α cluster decay theory

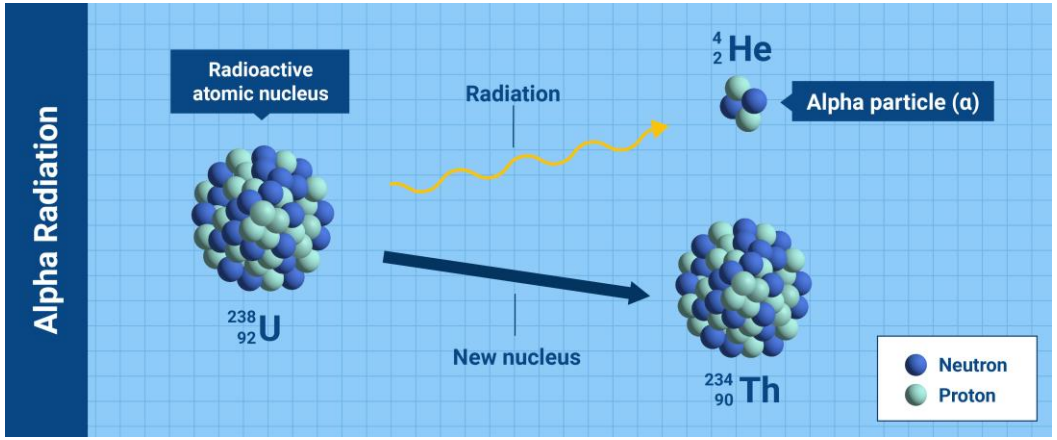

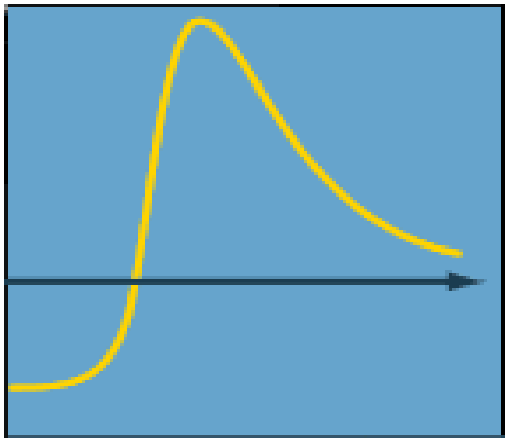

Old problem: one of the earliest and most convincing verifications of the validity of quantum mechanics

'Semi-classical' picture in textbooks: two-body tunneling problem by assuming an α cluster preformed inside the parent nucleus

α cluster preformation probability & frequency of collisions with barrier & probability of transmission through barrier

α cluster decay theory

α cluster decay: **at least a in-medium quantum four-body problem—cluster formation and dissolution, external interactions and strong Pauli blockings from the medium etc..**

Steps: **3-body in free space (t, ^{3}He); 4-body in free space (α); 3-α in free space (^{12}C); n/p+cluster in free space; 4-body in nuclei medium (α-decay)**

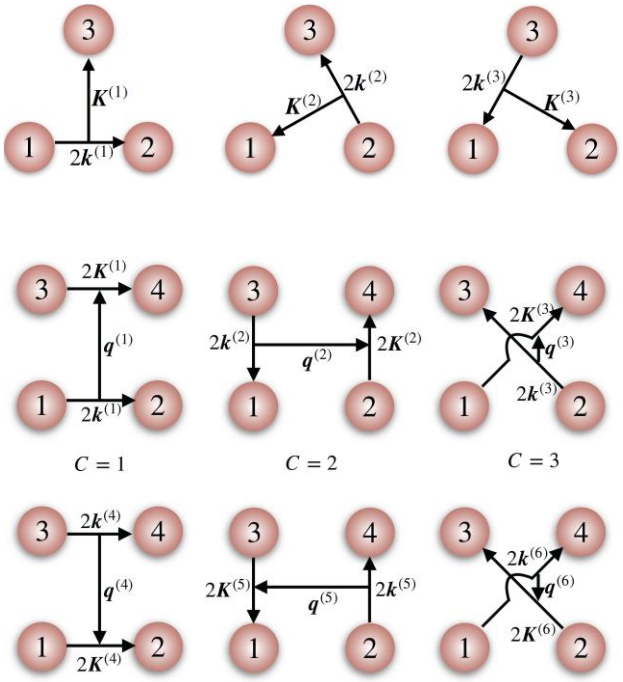

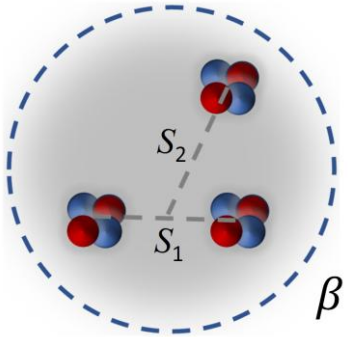

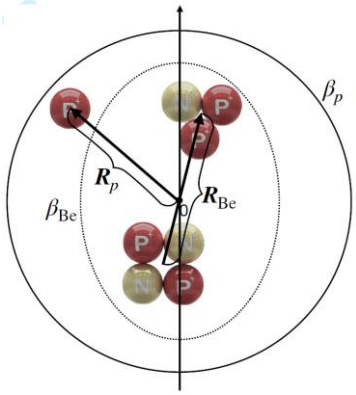

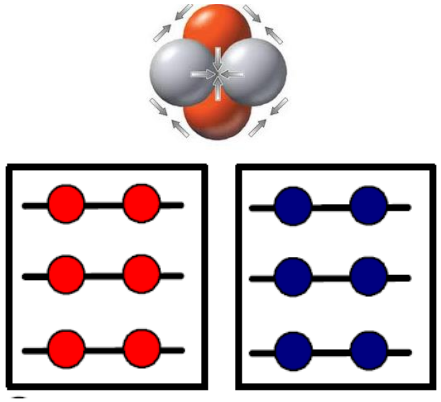

Quantum three-body problem (SRC)

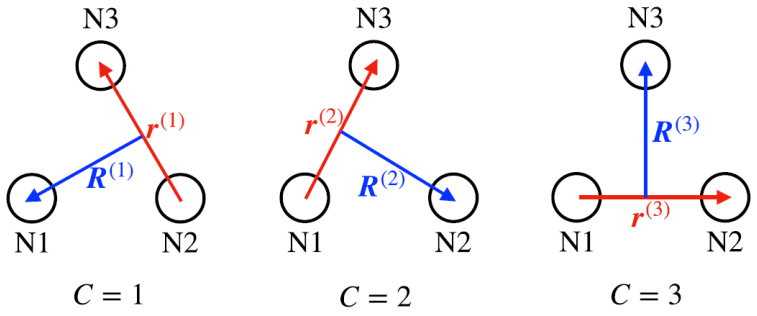

$$H = \sum_{i=1}^{3}\left(m_i + \frac{\boldsymbol{p}_i^2}{2m_i}\right) - T_G + \sum_{i<j=1}^{3} V_{ij} + V^{NNN}$$

$$\Psi_{TM_T,JM} = \sum_{C=1}\sum_{\alpha} A_\alpha \left[\left[\eta_{\frac{1}{2}}\eta_{\frac{1}{2}}\right]_t \eta_{\frac{1}{2}}\right]_{TM_T} \times \left[\left[\left[\chi_{\frac{1}{2}}\chi_{\frac{1}{2}}\right]_s \chi_{\frac{1}{2}}\right]_S \left[\phi_{nl}(\boldsymbol{r}^{(C)})\psi_{NL}(\boldsymbol{R}^{(C)})\right]_l\right]_{JM}$$

		Cal.(AV8′)	Cal.(AV8′+3NI)	Expt.
^{3}H	B.E. (MeV)	−7.77	−8.44	−8.48
	R_p (fm)	1.637	1.597	1.59
	R_n (fm)	1.790	1.740	
	R_{pn} (fm)	2.922	2.846	
	R_{nn} (fm)	3.189	3.094	
^{3}He	B.E. (MeV)	−7.11	−7.76	−7.72
	R_p (fm)	1.824	1.770	1.76
	R_n (fm)	1.660	1.617	
	R_{pn} (fm)	2.967	2.886	
	R_{pp} (fm)	3.256	3.152	

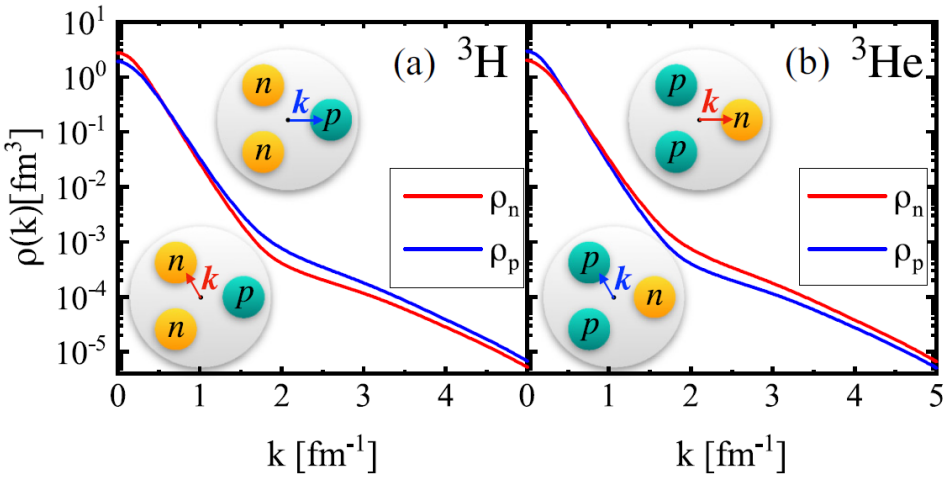

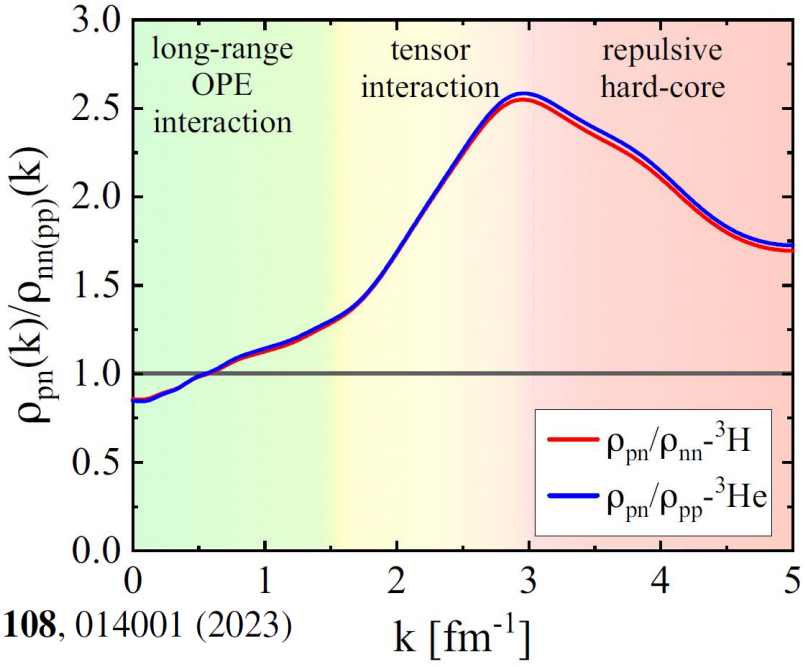

Qi Meng, Ziyang Lu, and Chang Xu* PHYSICAL REVIEW C **108**, 014001 (2023)

Single α cluster：quantum four-body problem

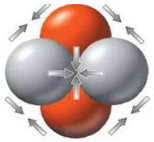

AV18

$$V_{ij} = \sum_{p=1,18} v_p(r_{ij}) O_{ij}^p$$

$$O_{ij}^{p=1,\ldots,14} = 1,\ \boldsymbol{\tau}_i \cdot \boldsymbol{\tau}_j,\ \boldsymbol{\sigma}_i \cdot \boldsymbol{\sigma}_j,\ (\boldsymbol{\sigma}_i \cdot \boldsymbol{\sigma}_j)(\boldsymbol{\tau}_i \cdot \boldsymbol{\tau}_j),$$
$$S_{ij},\ S_{ij}(\boldsymbol{\tau}_i \cdot \boldsymbol{\tau}_j),$$
$$\boldsymbol{L} \cdot \boldsymbol{S},\ \boldsymbol{L} \cdot \boldsymbol{S}(\boldsymbol{\tau}_i \cdot \boldsymbol{\tau}_j),$$
$$L^2,\ L^2(\boldsymbol{\tau}_i \cdot \boldsymbol{\tau}_j),\ L^2(\boldsymbol{\sigma}_i \cdot \boldsymbol{\sigma}_j),\ L^2(\boldsymbol{\sigma}_i \cdot \boldsymbol{\sigma}_j)(\boldsymbol{\tau}_i \cdot \boldsymbol{\tau}_j)$$
$$(\boldsymbol{L} \cdot \boldsymbol{S})^2,\ (\boldsymbol{L} \cdot \boldsymbol{S})^2(\boldsymbol{\tau}_i \cdot \boldsymbol{\tau}_j).$$

$$O_{ij}^{p=15,\ldots,18} = T_{ij},\ T_{ij}(\boldsymbol{\sigma}_i \cdot \boldsymbol{\sigma}_j),\ T_{ij}S_{ij},\ (\tau_{zi} + \tau_{zj})$$

AMD: $|\Psi_0\rangle = n_0 |\Psi_{\mathrm{AMD}}\rangle, \quad |\Psi_S\rangle = n_S F_S |\Psi_{\mathrm{AMD}}\rangle$

Central: $|\Psi_1\rangle = n_1 (1 - |\Psi_0\rangle \langle\Psi_0|) |\Psi_S\rangle,$

Tensor: $|\Psi_2\rangle = n_2 F_D |\Psi_0\rangle,$

Many-body: $|\Psi_3\rangle = n_3 (1 - |\Psi_0\rangle \langle\Psi_0| - |\Psi_1\rangle \langle\Psi_1| - |\Psi_2\rangle \langle\Psi_2|) |\Psi\rangle.$

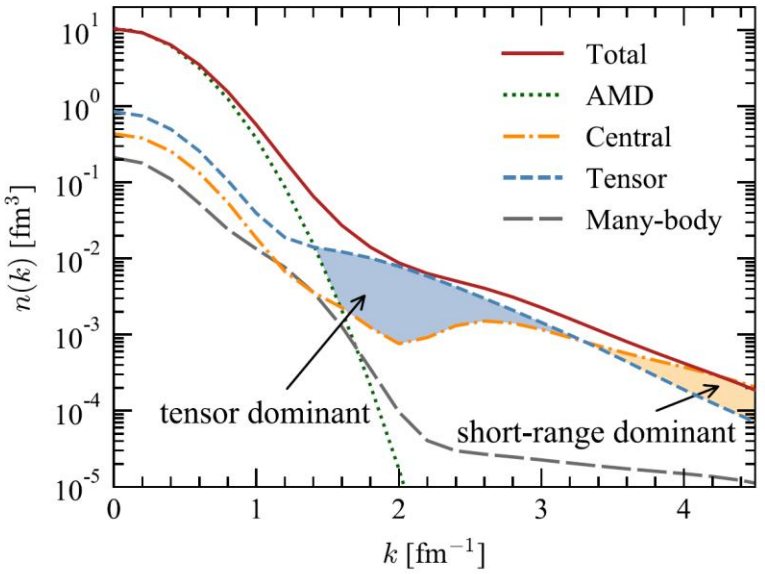

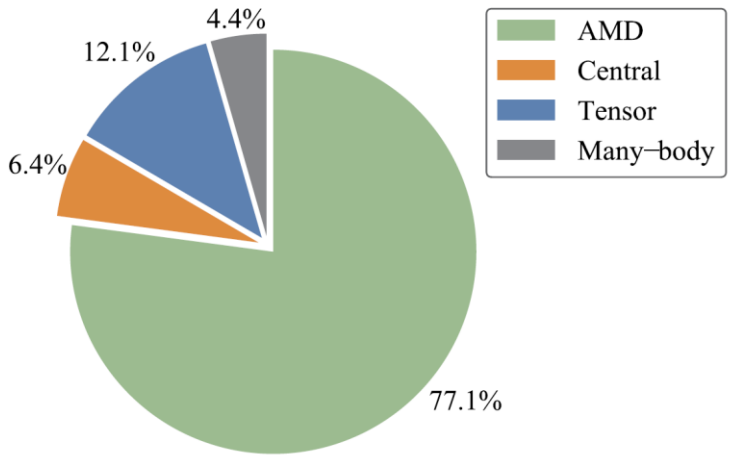

Lv... et.al *Physics Letters B 805 (2020) 135421*

Three α clusters: nonlocal motion

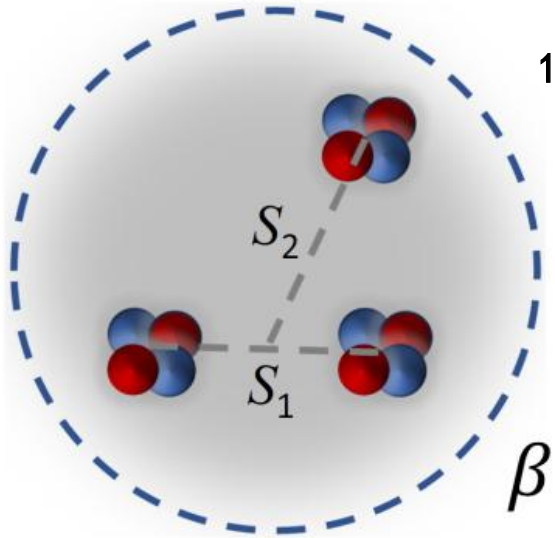

^{12}C: nonlocal motion and Pauli Blocking

$$\Phi(\boldsymbol{\beta}, \boldsymbol{S}_1, \boldsymbol{S}_2) = \int d^3R_1 d^3R_2 \exp\left[-\frac{(\boldsymbol{R}_1 - \boldsymbol{S}_1)^2}{2\boldsymbol{\beta}^2} - \frac{2(\boldsymbol{R}_2 - \boldsymbol{S}_2)^2}{3\boldsymbol{\beta}^2}\right]\Phi^B(\boldsymbol{R}_1, \boldsymbol{R}_2)$$

$$\propto \phi_G \mathcal{A}\left\{\exp\left[-\frac{(\boldsymbol{\xi}_1 - \boldsymbol{S}_1)^2}{B^2} - \frac{(\boldsymbol{\xi}_2 - \boldsymbol{S}_2)^2}{3/4\,B^2}\right]\phi(\alpha_1)\phi(\alpha_2)\phi(\alpha_3)\right\},$$

$$\Phi^B(\boldsymbol{R}_1, \boldsymbol{R}_2) \propto \phi_G \mathcal{A}\left\{\exp\left[-\frac{(\boldsymbol{\xi}_1 - \boldsymbol{R}_1)^2}{b^2} - \frac{(\boldsymbol{\xi}_2 - \boldsymbol{R}_2)^2}{3/4\,b^2}\right]\phi(\alpha_1)\phi(\alpha_2)\phi(\alpha_3)\right\},$$

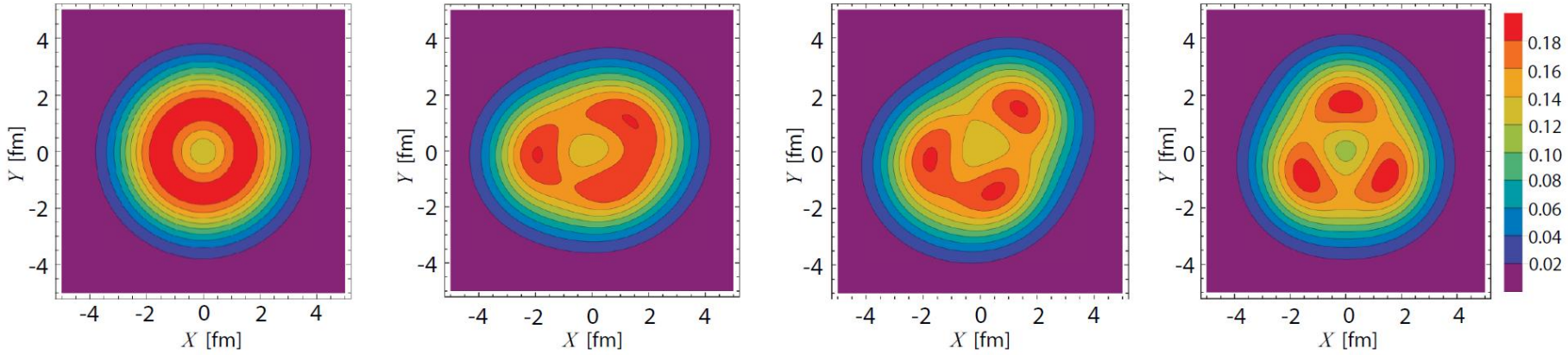

Zhou… et.al PHYSICAL REVIEW C **99**, 051303(R) (2019)

α cluster + ^{3}He + valence nucleon

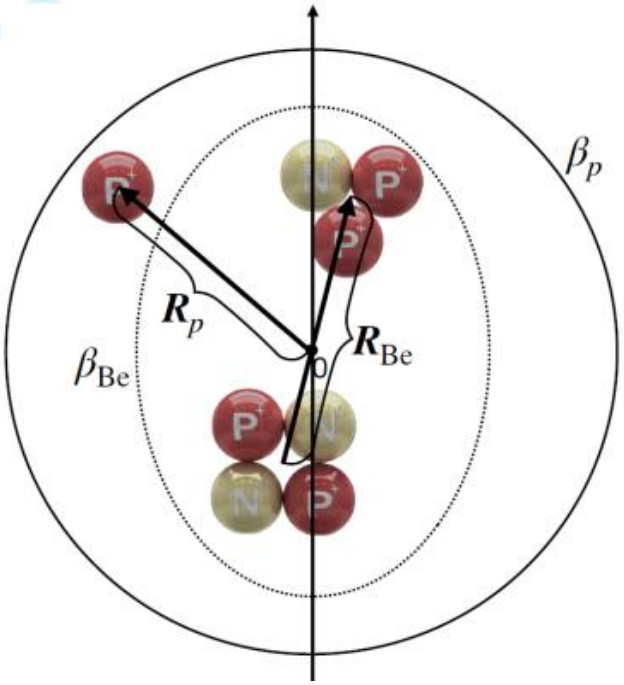

$$H = \sum_i^8 T_i - T_{c.m.} + \sum_{i<j}^8 V_{i,j}^N + \sum_{i<j}^8 V_{i,j}^C + \sum_{i<j}^8 V_{i,j}^{ls}$$

$$V_{ij}^N = \left\{ V_1 e^{-\alpha_1 r_{ij}^2} - V_2 e^{-\alpha_2 r_{ij}^2} \right\} \times \left\{ W - M\hat{P}_\sigma \hat{P}_\tau + B\hat{P}_\sigma - H\hat{P}_\tau \right\}$$

$$V_{ij}^{ls} = V_0^{ls} \left\{ e^{-\alpha_1 r_{ij}^2} - e^{-\alpha_2 r_{ij}^2} \right\} \mathbf{L} \cdot \mathbf{S} \hat{P}_{31}$$

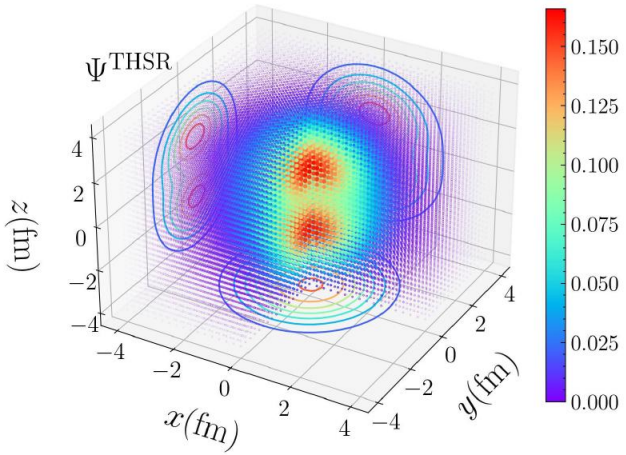

(a) Ψ^{THSR} matter density distribution

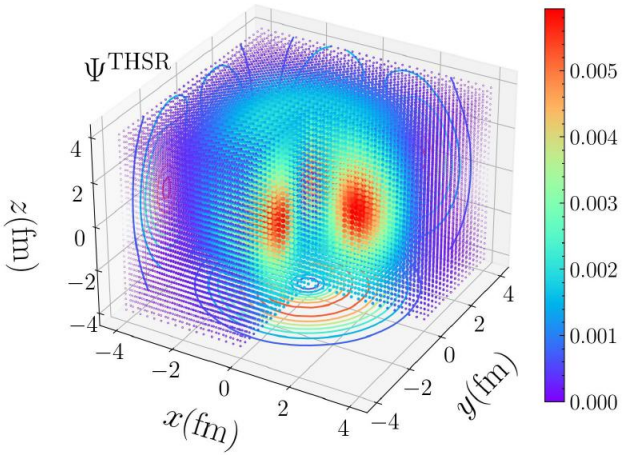

(b) Ψ^{THSR} valence density distribution

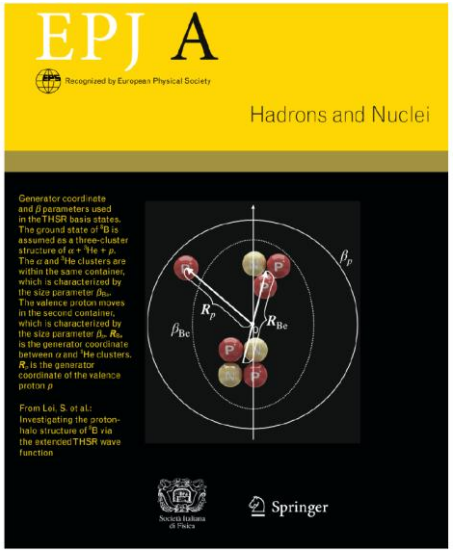

α cluster in nuclear medium

In-medium quantum four-body problem: α cluster formation & dissolution, external interactions and Pauli blockings

$^{104}Te \rightarrow {}^{100}Sn + \alpha$ — *N=Z=50*

$^{212}Po \rightarrow {}^{208}Pb + \alpha$ — *Z=82; N=126*

$^{274}Ds \rightarrow {}^{270}Hs + \alpha$ — *Z=108; N=162 (deformed)*

$^{302}Lv \rightarrow {}^{298}Fl + \alpha$ — *Z=114; N=184*

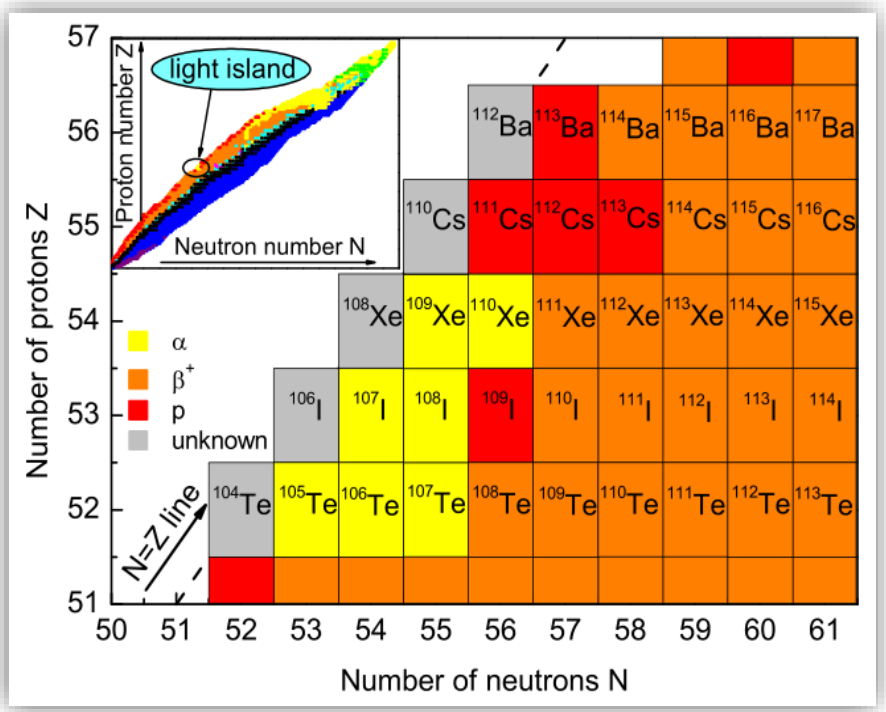

^{104}Te

Enhanced clustering?

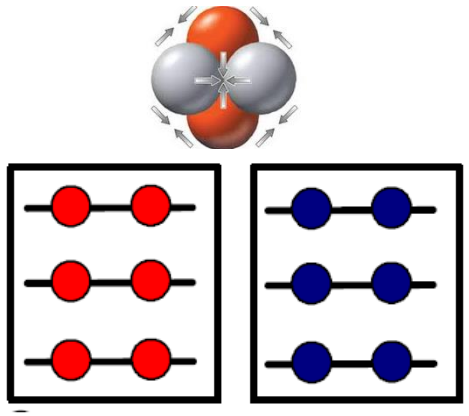

α cluster + doubly magic core ^{100}Sn

^{104}Te

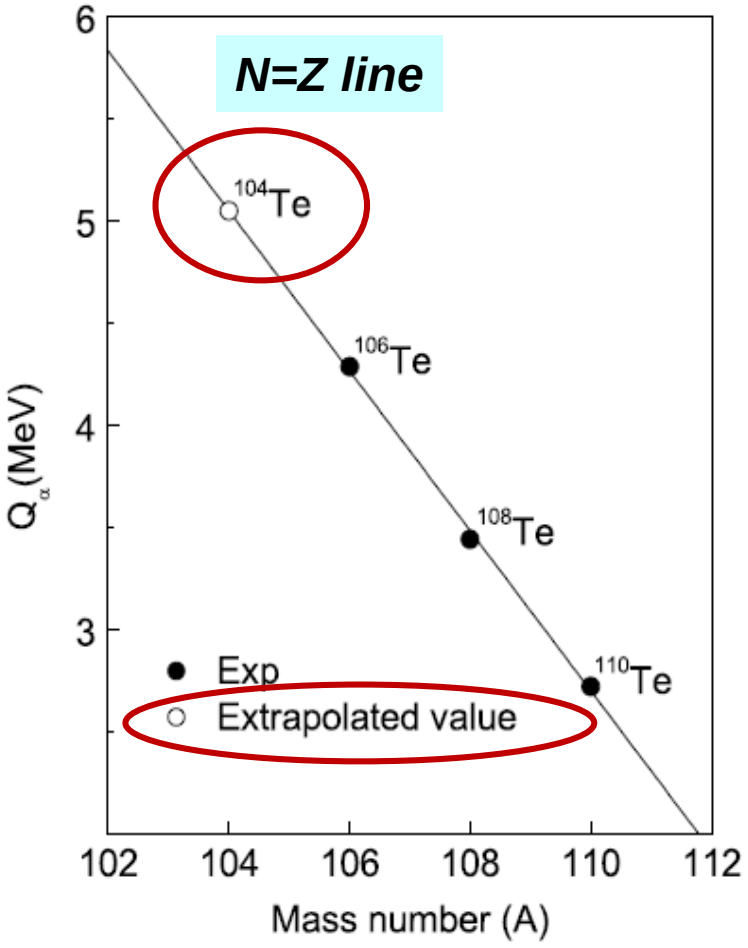

Decay energy extrapolation

Decay half-life prediction

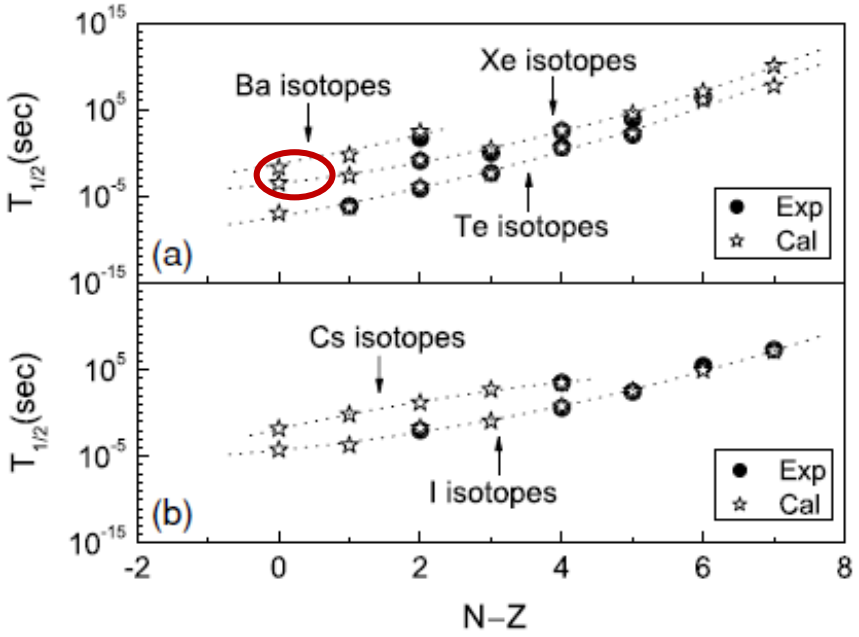

asymmetry along the isotopic chains [7]. To improve the agreement between experiment and theory, we therefore use the isospin-dependent preformation factor $P_\alpha = c_1 + c_2(N - Z)$ instead of the constant one [19] for each kind of nuclei [e.g., a linear dependence $P_\alpha^{ee} = 0.73 - 0.09 \times (N - Z)$ for the even-even nuclei]. As expected, the corresponding theoretical

C. Xu and Z. Ren, Phys. Rev. C **74**, 037302 (2006).

PHYSICAL REVIEW C 77, 034301 (2008)

University of Tennessee

Toward ^{100}Sn: Studies of excitation functions for the reaction between ^{58}Ni and ^{54}Fe ions

A. Korgul,[1,2,3,4] K. P. Rykaczewski,[5] C. J. Gross,[5] R. K. Grzywacz,[3] S. N. Liddick,[3,6] C. Mazzocchi,[3,7] J. C. Batchelder,[8] C. R. Bingham,[3] I. G. Darby,[3] C. Goodin,[4] J. H. Hamilton,[4] J. K. Hwang,[4] S. V. Ilyushkin,[9] W. Królas,[10] and J. A. Winger[2,8,11]

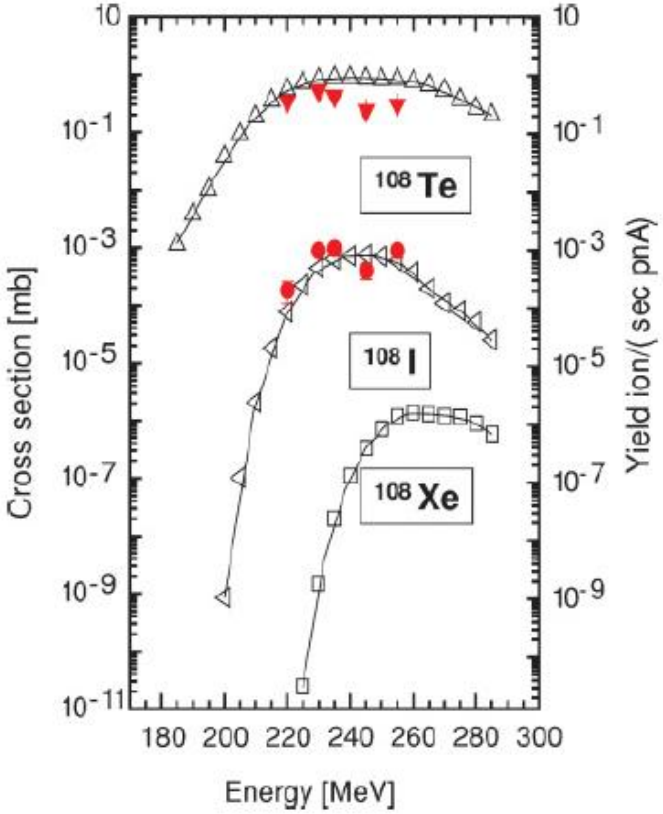

beam energy around 240 MeV will maximize the production of the $A = 108$ isobar ^{108}Xe in the ^{58}Ni+^{54}Fe reaction. The cross section for the $4n$ evaporation channel can be expected at the (sub)nanobarn level, see Fig. 4. At $\sigma = 1$ nb, the implantation of about 20 ^{108}Xe ions can be achieved in 100 hr with 50 pnA beam intensity and a 300 μg/cm^2 ^{54}Fe target. The targets rotating with the speed corresponding to a linear velocity for the irradiated spot of about 0.3 m/s can withstand this high beam intensity, see, e.g., Ref. [32]. The predicted half-lives of ^{108}Xe and ^{104}Te are of the order of 50 μs and 10 ns, respectively [14,15]. Using digital pulse processing and recording decay signal waveforms, one should be able to identify the pileup of two α signals at the sum energy around 10 MeV [15].

Decay half-life prediction: 10ns

[14] C. Xu and Z. Ren, Phys. Rev. C **74**, 037302 (2006).
[15] P. Mohr, Eur. Phys. J. A **31**, 23 (2007).

Editors' Suggestion | Featured in Physics

Superallowed α Decay to Doubly Magic ^{100}Sn

K. Auranen,[1,*] D. Seweryniak,[1] M. Albers,[1] A. D. Ayangeakaa,[1,†] S. Bottoni,[1,‡] M. P. Carpenter,[1] C. J. Chiara,[1,2,§] P. Copp,[1,3] H. M. David,[1,‖] D. T. Doherty,[4,¶] J. Harker,[1,2] C. R. Hoffman,[1] R. V. F. Janssens,[5,6] T. L. Khoo,[1] S. A. Kuvin,[1,7] T. Lauritsen,[1] G. Lotay,[8] A. M. Rogers,[1,**] J. Sethi,[1,2] C. Scholey,[9] R. Talwar,[1] W. B. Walters,[2] P. J. Woods,[4] and S. Zhu[1]

[1]*Physics Division, Argonne National Laboratory, 9700 South Cass Avenue, Lemont, Illinois 60439, USA*
[2]*Department of Chemistry and Biochemistry, University of Maryland, College Park, Maryland 20742, USA*
[3]*Department of Physics and Applied Physics, University of Massachusetts Lowell, Lowell, Massachusetts 01854, USA*
[4]*University of Edinburgh, Edinburgh EH9 3JZ, United Kingdom*
[5]*Department of Physics and Astronomy, University of North Carolina at Chapel Hill, Chapel Hill, North Carolina 27599, USA*
[6]*Triangle Universities Nuclear Laboratory, Duke University, Durham, North Carolina 27708, USA*
[7]*Department of Physics, University of Connecticut, Storrs, Connecticut 06269, USA*
[8]*University of Surrey, Guildford GU2 7XH, United Kingdom*
[9]*Department of Physics, University of Jyvaskyla, P.O. Box 35, FI-40014 University of Jyvaskyla, Finland*

(Received 31 July 2018; revised manuscript received 7 September 2018; published 30 October 2018)

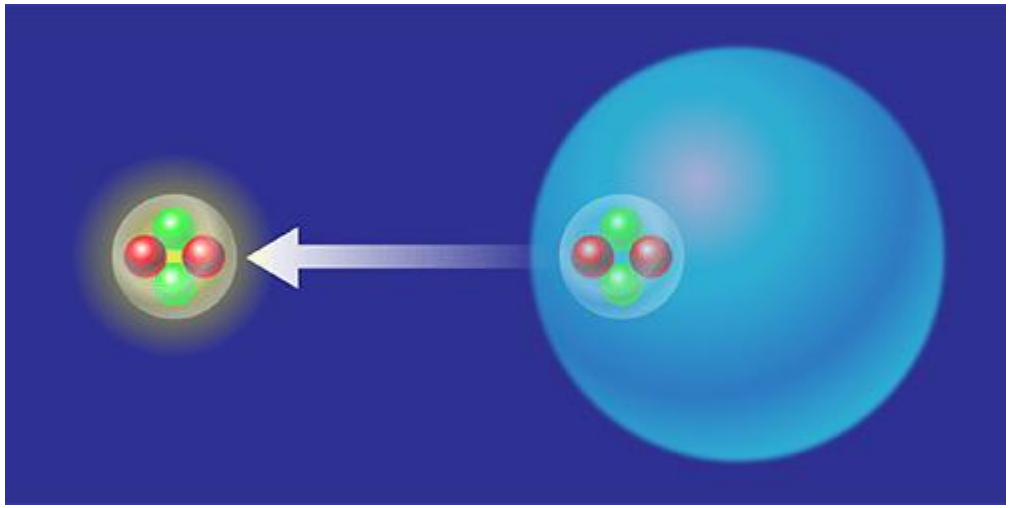

The Fastest Alpha Emitter

"Tellurium-104 is now also the fastest known alpha emitter—though this finding is more fun than fundamental."

PHYSICAL REVIEW LETTERS **121,** 182501 (2018)

Editors' Suggestion | Featured in Physics

Superallowed α Decay to Doubly Magic ^{100}Sn

Chain	Nuclide	E_α (keV)	$T_{1/2}$	b_α (%)
$N = Z$	^{108}Xe	4400(200)	58^{+106}_{-23} μs	100[a]
$N = Z$	^{104}Te	4900(200)	<18 ns	100[a]
$N = Z + 2$	^{114}Ba	3480(20) [17]	380^{+190}_{-110} ms [17]	0.9(3) [35]
$N = Z + 2$	^{110}Xe	3720(20) [17]	95^{+25}_{-20} ms [17]	64(35) [35]
$N = Z + 2$	^{106}Te	4128(9) [36]	70^{+20}_{-15} μs [17]	100 [35]
$N = Z + 4$	^{112}Xe	3216(7) [36]	2.7(8) s [37]	$0.8^{+1.1}_{-0.5}$ [36]
$N = Z + 4$	^{108}Te	3314(4) [20]	2.1(1) s [37]	49(4) [36]

suddenly. The present data are in agreement with this linear trend, and therefore with the extrapolated values of $Q_\alpha(^{104}\mathrm{Te}) = 5.053$ MeV and $Q_\alpha(^{108}\mathrm{Xe}) = 4.440$ MeV [29]. Furthermore, the folding potential calculations

[29] C. Xu and Z. Ren, Phys. Rev. C **74**, 037302 (2006).

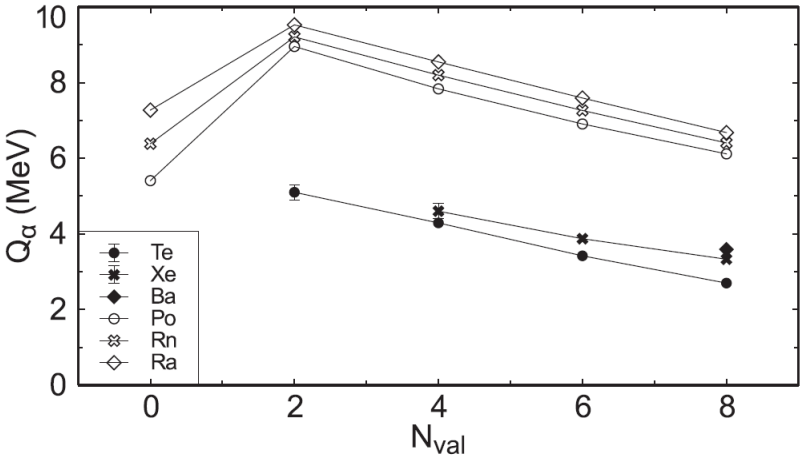

Synopsis: The Fastest Alpha Emitter

October 30, 2018

The detection of unusually fast alpha emission from a heavy isotope could lead to new ways of testing the nuclear shell model.

with iron. They then looked for two alpha particles: one from xenon-108 decaying to tellurium-104, the other from tellurium-104 decaying to tin-100. So far, they have detected two of these double-alpha events, and they have placed an upper limit of 18 ns on the tellurium-104 half-life. The measured lifetime limit is in line with shell-model calculations, which predict that alpha preformation in tellurium-104 is several times more likely than in the alpha emitter polonium-212, a benchmark for shell-model calculations. Tellurium-104 is now also the fastest known alpha emitter—though this finding is more fun than fundamental. **2018: ^{104}Te <18ns (experiment)**

Fastest α emitter ^{104}Te

PHYSICAL REVIEW C **100**, 034315 (2019)

Search for α decay of ^{104}Te with a novel recoil-decay scintillation detector

Y. Xiao,[1] S. Go,[1,2] R. Grzywacz,[1,3] R. Orlandi,[4] A. N. Andreyev,[4,5] M. Asai,[4] M. A. Bentley,[5] G. de Angelis,[6] C. J. Gross,[3] P. Hausladen,[3] K. Hirose,[4] S. Hofmann,[7] H. Ikezoe,[4] D. G. Jenkins,[5] B. Kindler,[7] R. Léguillon,[4] B. Lommel,[7] H. Makii,[4] C. Mazzocchi,[8] K. Nishio,[4] P. Parkhurst,[9] S. V. Paulauskas,[1] C. M. Petrache,[10] K. P. Rykaczewski,[3] T. K. Sato,[4] J. Smallcombe,[4] A. Toyoshima,[4] K. Tsukada,[4] K. Vaigneur,[11] and R. Wadsworth[5]

[1]*Department of Physics and Astronomy, University of Tennessee, Knoxville, Tennessee 37996, USA*

[2]*Department of Physics, Kyushu University, Fukuoka 819-0395, Japan*

[3]*Physics Division, Oak Ridge National Laboratory, Oak Ridge, Tennessee 37831, USA*

[4]*Advanced Science Research Center, Japan Atomic Energy Agency, Tokai, Ibaraki 319-1195, Japan*

[5]*Department of Physics, University of York, Heslington, York YO10 5DD, United Kingdom*

[6]*Istituto Nazionale di Fisica Nucleare - Laboratori Nazionali di Legnaro, Legnaro PD 35020, Italy*

[7]*GSI Helmholtz Centre for Heavy Ion Research, Darmstadt 64291, Germany*

[8]*Faculty of Physics, University of Warsaw, Warszawa PL 02-093, Poland*

[9]*Proteus, Inc., Chagrin Falls, Ohio 44022, USA*

[10]*Centre de Sciences Nucléaires et Sciences de la Matiére, CNRS/IN2P3, Université Paris-Saclay, 91405 Orsay, France*

[11]*Agile Technologies, Knoxville, Tennessee 37932, USA*

(Received 5 August 2018; revised manuscript received 31 July 2019; published 16 September 2019)

Search for α decay of ^{104}Te with a novel recoil-decay scintillation detector

Y. Xiao,[1] S. Go,[1,2] R. Grzywacz,[1,3] R. Orlandi,[4] A. N. Andreyev,[4,5] M. Asai,[4] M. A. Bentley,[5] G. de Angelis,[6] C. J. Gross,[3] P. Hausladen,[3] K. Hirose,[4] S. Hofmann,[7] H. Ikezoe,[4] D. G. Jenkins,[5] B. Kindler,[7] R. Léguillon,[4] B. Lommel,[7] H. Makii,[4] C. Mazzocchi,[8] K. Nishio,[4] P. Parkhurst,[9] S. V. Paulauskas,[1] C. M. Petrache,[10] K. P. Rykaczewski,[3] T. K. Sato,[4] J. Smallcombe,[4] A. Toyoshima,[4] K. Tsukada,[4] K. Vaigneur,[11] and R. Wadsworth[5]

I. INTRODUCTION

In the α-decay island northeast of ^{100}Sn, valence protons and neutrons are expected to occupy the same single-particle orbitals outside the $N = Z = 50$ doubly magic nucleus ^{100}Sn. The additional interaction between protons and neutrons may lead to the enhanced pre-formation of an α particle and therefore to the enhancement of α-decay probability, the so-called superallowed α decay [1]. Extensive experimental efforts have been made in this region, providing evidence of such enhancement [2–6]. The ultimate evidence would be the observation of accelerated α decay of ^{104}Te ($N = Z = 52$) with two protons and two neutrons occupying the same single-particle orbitals. When α clusterization is included, the estimated half-life would be as short as 50 ns [7], which makes the measurement of ^{104}Te decay very difficult. The indirect production of this isotope through the synthesis of the longer-lived α-decay precursor ^{108}Xe, whose half-life is estimated to be 0.15 ms [7] by the same model with enhanced preformation, would enable the study of ^{104}Te using the in-flight electromagnetic separation technique. Even in this case, the short half-life of ^{104}Te is a challenge for today's detection techniques and requires the use of a fast response detection method to be able to separate the α decay of ^{108}Xe and the fast α decay of ^{104}Te. Semiconductor detectors, e.g., double-sided strip detectors (DSSDs), are widely used as implantation detectors for such measurements of ions and charged particle emission. One of the shortcoming of semiconductor detector

The short half-life of 104Te: challenge for today's detection techniques

to radiation damage. A recent measurement [10] resulted with the half-life estimate $T_{1/2} < 18$ ns for ^{104}Te based on

[7] C. Xu and Z. Ren, Phys. Rev. C **74**, 037302 (2006).

α cluster + a doubly magic core ^{100}Sn

PHYSICAL REVIEW C **100**, 034315 (2019)

Search for α decay of ^{104}Te with a novel recoil-decay scintillation detector

Y. Xiao,[1] S. Go,[1,2] R. Grzywacz,[1,3] R. Orlandi,[4] A. N. Andreyev,[4,5] M. Asai,[4] M. A. Bentley,[5] G. de Angelis,[6] C. J. Gross,[3] P. Hausladen,[3] K. Hirose,[4] S. Hofmann,[7] H. Ikezoe,[4] D. G. Jenkins,[5] B. Kindler,[7] R. Léguillon,[4] B. Lommel,[7] H. Makii,[4] C. Mazzocchi,[8] K. Nishio,[4] P. Parkhurst,[9] S. V. Paulauskas,[1] C. M. Petrache,[10] K. P. Rykaczewski,[3] T. K. Sato,[4] J. Smallcombe,[4] A. Toyoshima,[4] K. Tsukada,[4] K. Vaigneur,[11] and R. Wadsworth[5]

[1]*Department of Physics and Astronomy, University of Tennessee, Knoxville, Tennessee 37996, USA*

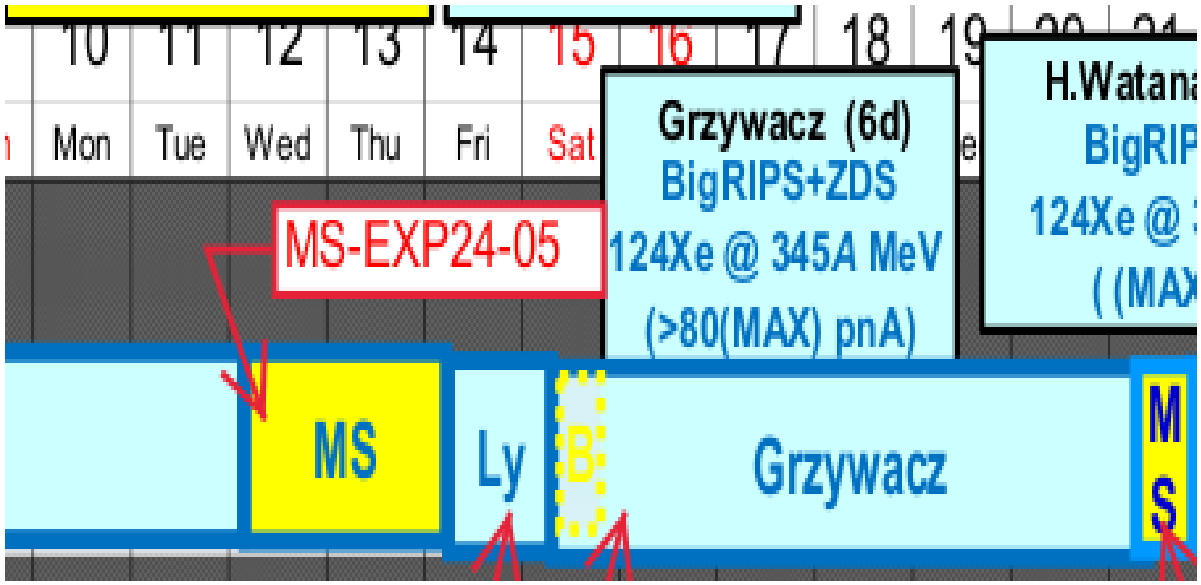

Robert Grzywacz

Professor

Director, UT-ORNL Joint Institute for Nuclear Physics & Applications

Experimental Nuclear Physics

Office: 613 Science and Engineering Research Facility/ORNL

Phone: 974-2918 or 574-4732

rgrzywac@utk.edu

α cluster + a doubly magic core ^{208}Pb

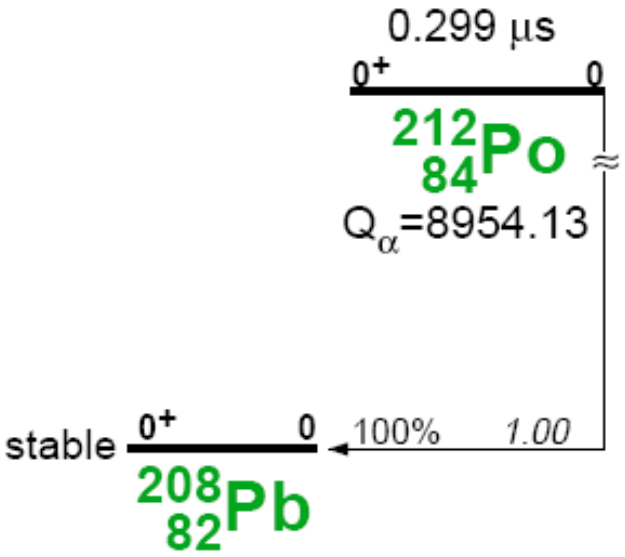

Spherical

Doubly magic

Only one decay channel

Accurate experimental data

……

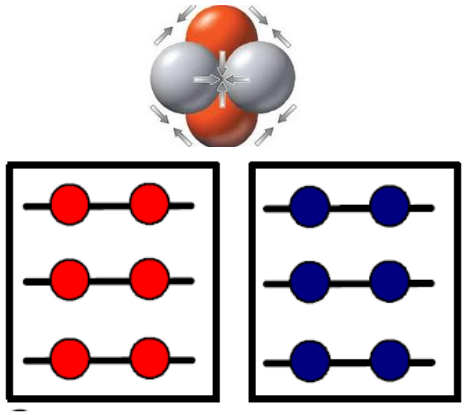

Microscopic calculation of alpha cluster formation and decay in ^{212}Po

Alpha cluster formation and decay

——*Quartetting wave function approach*

Quantum few-body problem (2p+2n+core)

Subdivide the W.F. into an intrinsic part and a c.o.m part

$$\Psi(\mathbf{R},\mathbf{s}_j) = \varphi^{\text{intr}}(\mathbf{s}_j,\mathbf{R})\,\Phi(\mathbf{R})$$

$$\begin{aligned}
\mathbf{r}_{n,\uparrow} &= \mathbf{R} + \mathbf{S}/2 + \mathbf{s}/2 \\
\mathbf{r}_{n,\downarrow} &= \mathbf{R} + \mathbf{S}/2 - \mathbf{s}/2 \\
\mathbf{r}_{p,\uparrow} &= \mathbf{R} - \mathbf{S}/2 + \mathbf{s}'/2 \\
\mathbf{r}_{p,\downarrow} &= \mathbf{R} - \mathbf{S}/2 - \mathbf{s}'/2
\end{aligned}$$

equation for the c.m. motion

$$-\frac{\hbar^2}{2Am}\nabla_R^2\Phi(\mathbf{R}) - \frac{\hbar^2}{Am}\int ds_j \varphi^{\text{intr},*}(\mathbf{s}_j,\mathbf{R})[\nabla_R\varphi^{\text{intr}}(\mathbf{s}_j,\mathbf{R})][\nabla_R\Phi(\mathbf{R})]$$

$$-\frac{\hbar^2}{2Am}\int ds_j \varphi^{\text{intr},*}(\mathbf{s}_j,\mathbf{R})\left[\nabla_R^2\varphi^{\text{intr}}(\mathbf{s}_j,\mathbf{R})\right]\Phi(\mathbf{R}) + \int dR'\, W(\mathbf{R},\mathbf{R}')\Phi(\mathbf{R}') = E\,\Phi(\mathbf{R})$$

equation for the intrinsic motion

$$-\frac{\hbar^2}{Am}\Phi^*(\mathbf{R})[\nabla_R\Phi(\mathbf{R})][\nabla_R\varphi^{\text{intr}}(\mathbf{s}_j,\mathbf{R})] - \frac{\hbar^2}{2Am}|\Phi(\mathbf{R})|^2\nabla_R^2\varphi^{\text{intr}}(\mathbf{s}_j,\mathbf{R})$$

$$+\int dR'\,ds'_j\,\Phi^*(\mathbf{R})\left\{T\left[\nabla_{s_j}\right]\delta(\mathbf{R}-\mathbf{R}')\delta(\mathbf{s}_j-\mathbf{s}'_j) + V(\mathbf{R},\mathbf{s}_j;\mathbf{R}',\mathbf{s}'_j)\right\}\Phi(\mathbf{R}')\varphi^{\text{intr}}(\mathbf{s}'_j,\mathbf{R}') = F(\mathbf{R})\varphi^{\text{intr}}(\mathbf{s}_j,\mathbf{R})$$

Alpha cluster formation and decay

——*Quartetting wave function approach*

$$\mathbf{p}_1 = \mathbf{P}/4 + \mathbf{k}/2 + \mathbf{k}_{12}, \qquad \mathbf{p}_2 = \mathbf{P}/4 + \mathbf{k}/2 - \mathbf{k}_{12},$$
$$\mathbf{p}_3 = \mathbf{P}/4 - \mathbf{k}/2 + \mathbf{k}_{34}, \qquad \mathbf{p}_4 = \mathbf{P}/4 - \mathbf{k}/2 - \mathbf{k}_{34}.$$

$$\frac{\hbar^2}{2m}[k^2 + 2k_{12}^2 + 2k_{34}^2]\tilde{\varphi}^{\text{intr}}(\mathbf{k}, \mathbf{k}_{12}, \mathbf{k}_{34}, \mathbf{P}) +$$
$$\int \frac{d^3k'}{(2\pi)^3}\frac{d^3k'_{12}}{(2\pi)^3}\frac{d^3k'_{34}}{(2\pi)^3}\tilde{V}_4(\mathbf{k}, \mathbf{k}_{12}, \mathbf{k}_{34}; \mathbf{k}', \mathbf{k}'_{12}, \mathbf{k}'_{34}; \mathbf{P})\tilde{\varphi}^{\text{intr}}(\mathbf{k}', \mathbf{k}'_{12}, \mathbf{k}'_{34}, \mathbf{P})$$
$$= \tilde{W}(\mathbf{P})\tilde{\varphi}^{\text{intr}}(\mathbf{k}, \mathbf{k}_{12}, \mathbf{k}_{34}, \mathbf{P})$$

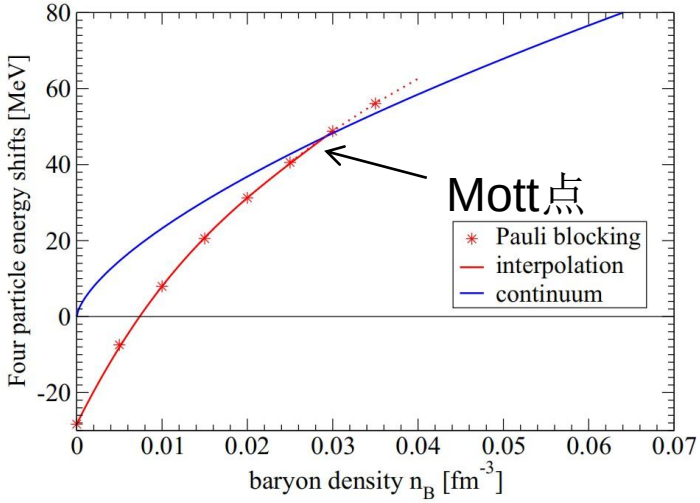

$$\tilde{W}^{\text{intr}}(\mathbf{P}) = \frac{\hbar^2}{2m}\int \frac{d^3k}{(2\pi)^3}\frac{d^3k_{12}}{(2\pi)^3}\frac{d^3k_{34}}{(2\pi)^3}\left[k^2 + 2k_{12}^2 + 2k_{34}^2\right]|\tilde{\varphi}^{\text{intr}}(\mathbf{k}, \mathbf{k}_{12}, \mathbf{k}_{34}, \mathbf{P})|^2$$
$$+ \int \frac{d^3k}{(2\pi)^3}\frac{d^3k_{12}}{(2\pi)^3}\frac{d^3k_{34}}{(2\pi)^3}\frac{d^3k'}{(2\pi)^3}\frac{d^3k'_{12}}{(2\pi)^3}\frac{d^3k'_{34}}{(2\pi)^3}\tilde{\varphi}^{\text{intr},*}(\mathbf{k}, \mathbf{k}_{12}, \mathbf{k}_{34}, \mathbf{P})$$
$$\times\tilde{V}_4^{\text{intr}}(\mathbf{k}, \mathbf{k}_{12}, \mathbf{k}_{34}; \mathbf{k}', \mathbf{k}'_{12}, \mathbf{k}'_{34}; \mathbf{P})\tilde{\varphi}^{\text{intr}}(\mathbf{k}', \mathbf{k}'_{12}, \mathbf{k}'_{34}, \mathbf{P})$$

$$\tilde{W}^{\text{intr,bound}}(n_B) = \tilde{W}^{\text{Pauli}}(n_B) - 28.3\,\text{MeV}$$

$$\tilde{W}^{\text{intr,free}}(n_B) = 2E_{\text{Fermi}}(n_n) + 2E_{\text{Fermi}}(n_p) = \frac{\hbar^2}{m}\left[2(\frac{3}{2}\pi^2 n_B)^{2/3}\right]$$

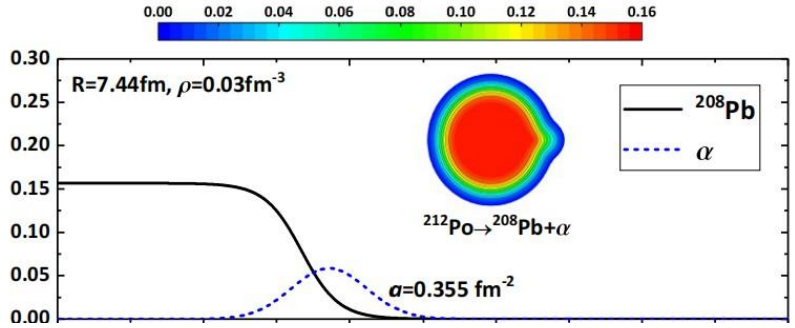

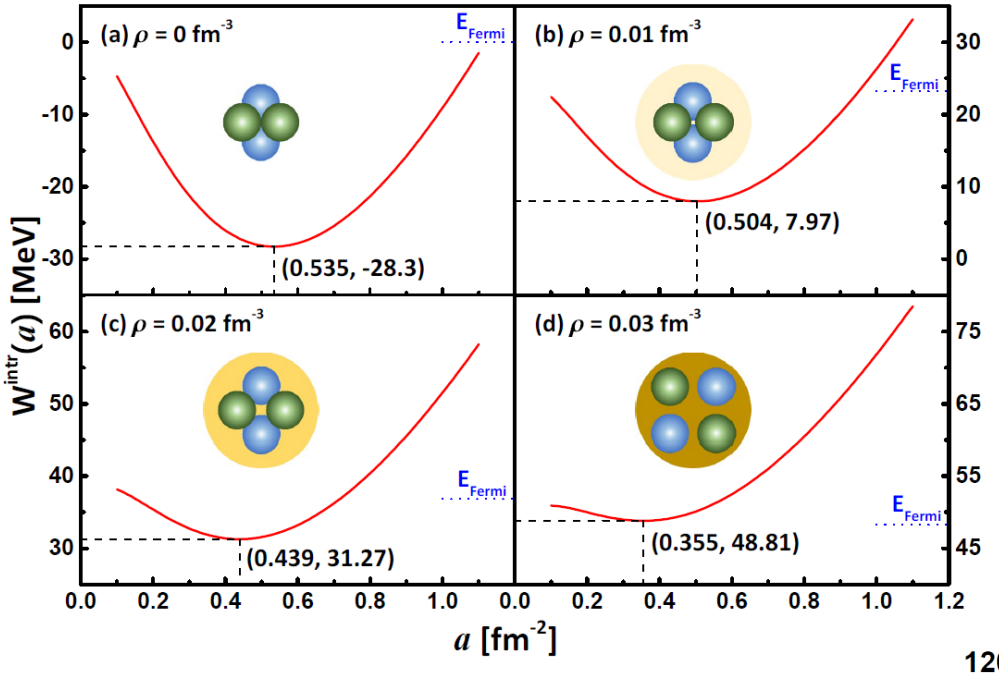

Strong binding of α-cluster is gradually reduced

Energy shift due to Pauli blocking after it feels the tail of the core density

Eventually α-cluster dissolves. Before that, remains a relatively compact entity with small extension even up to the critical density

Four nucleons go over into single particle states with pair correlations in the open shells on top of the core

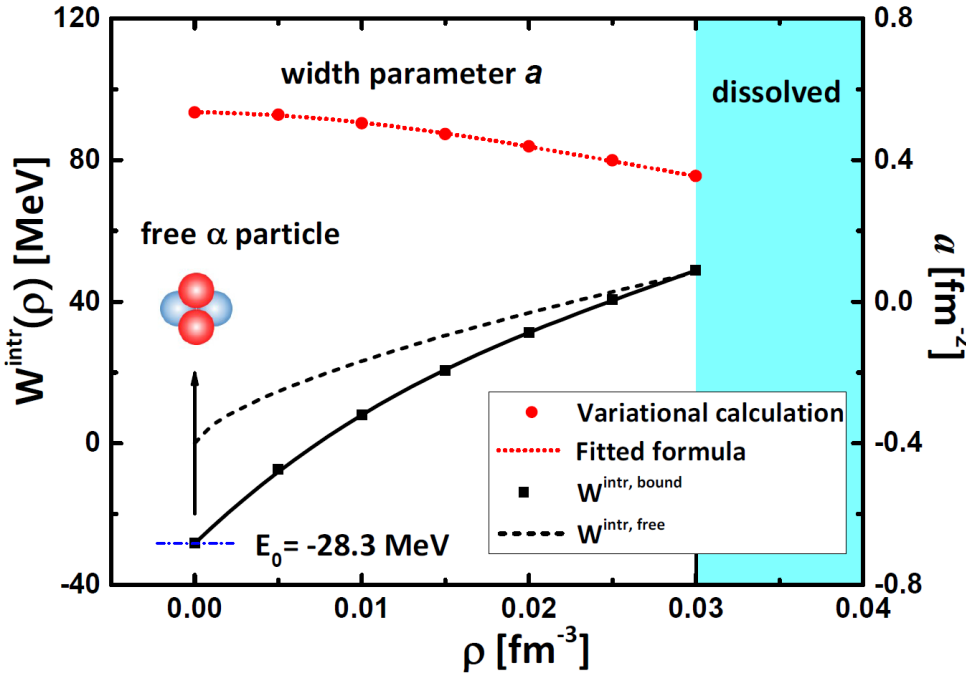

Alpha cluster formation and decay

——*Quartetting wave function approach*

Intrinsic bound-state W. F. transforms at critical density into an unbound 4 nucleon shell-model state

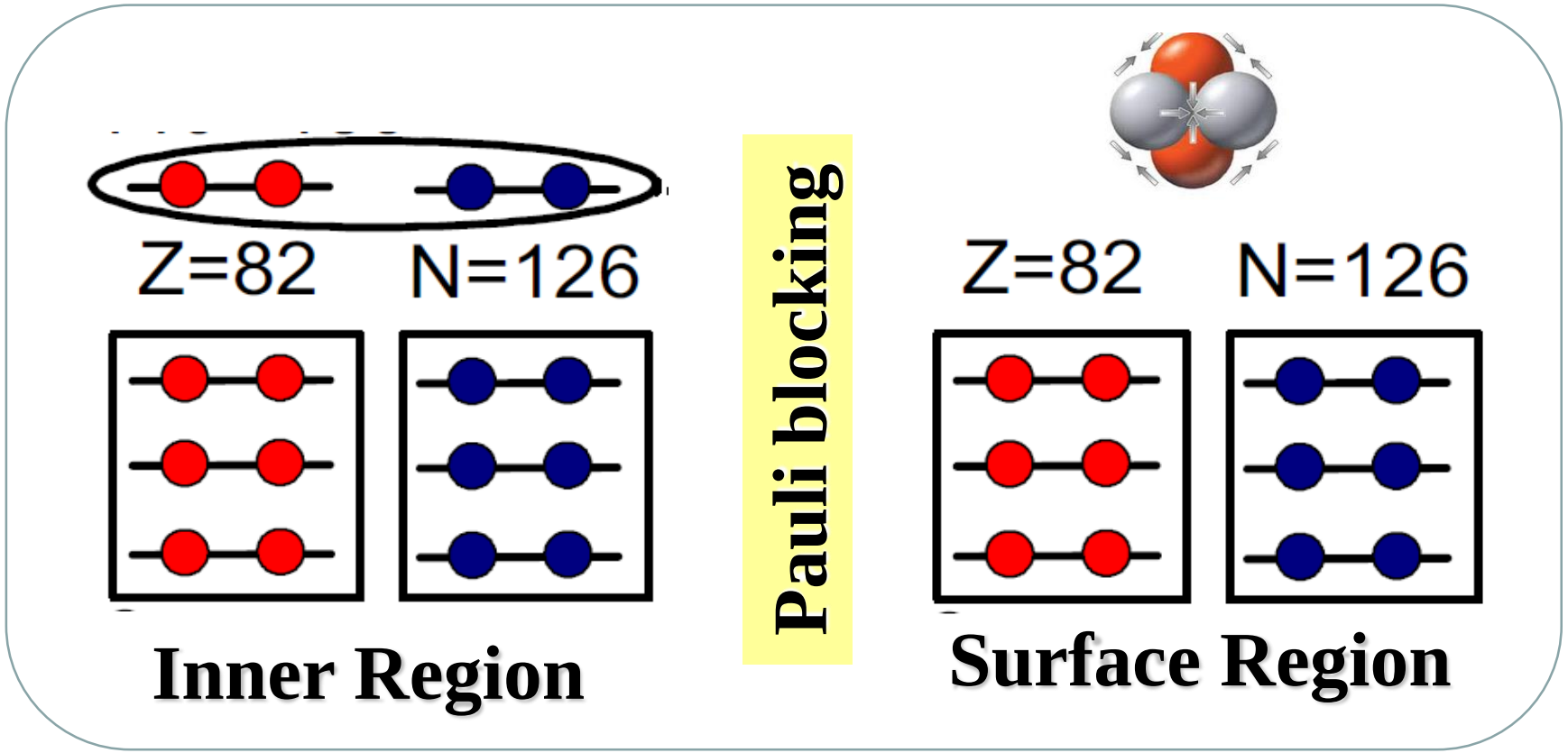

Alpha cluster formation and decay

——*Quartetting wave function approach*

$$\left\langle \varphi_\alpha^{\rm intr} | \varphi_{\rm quartet}^{\rm intr} \right\rangle (R) = \int d^3S\, d^3s\, d^3s'\, \varphi_\alpha^{\rm intr,*}(\mathbf{S},\mathbf{s},\mathbf{s}') \varphi_{\rm quartet}^{\rm intr}(\mathbf{R},\mathbf{S},\mathbf{s},\mathbf{s}')$$

$$= \int d^3S\, d^3s\, d^3s'\, \frac{\mathscr{Y}_\alpha^*(\mathbf{r_1})\mathscr{Y}_\alpha^*(\mathbf{r_2})\mathscr{Y}_\alpha^*(\mathbf{r_3})\mathscr{Y}_\alpha^*(\mathbf{r_4})\Phi_{\rm quartet}(\mathbf{R},\mathbf{S},\mathbf{s},\mathbf{s}')}{\mathscr{Z}_\alpha^*(\mathbf{R})\Psi_{\rm quartet}^{\rm com}(\mathbf{R})}$$

$$= \frac{64(2\pi)^9}{\mathscr{Z}_\alpha(\mathbf{R})\Psi_{\rm quartet}^{\rm com}(\mathbf{R})} \int d^3p\, \phi_{12}(\mathbf{p})\phi_{34}(\mathbf{p}) e^{i\mathbf{p}\cdot\mathbf{R}}.$$

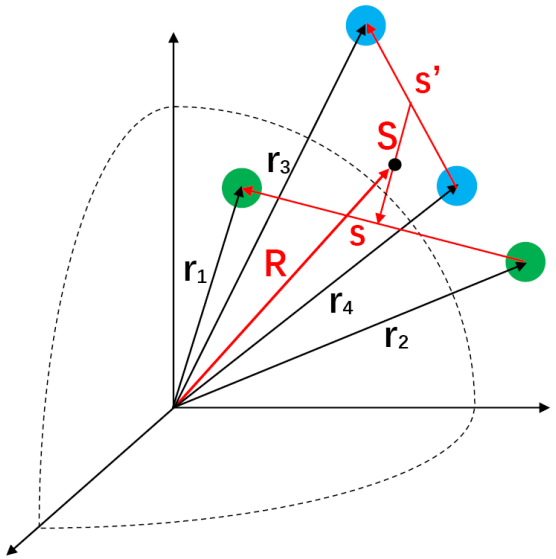

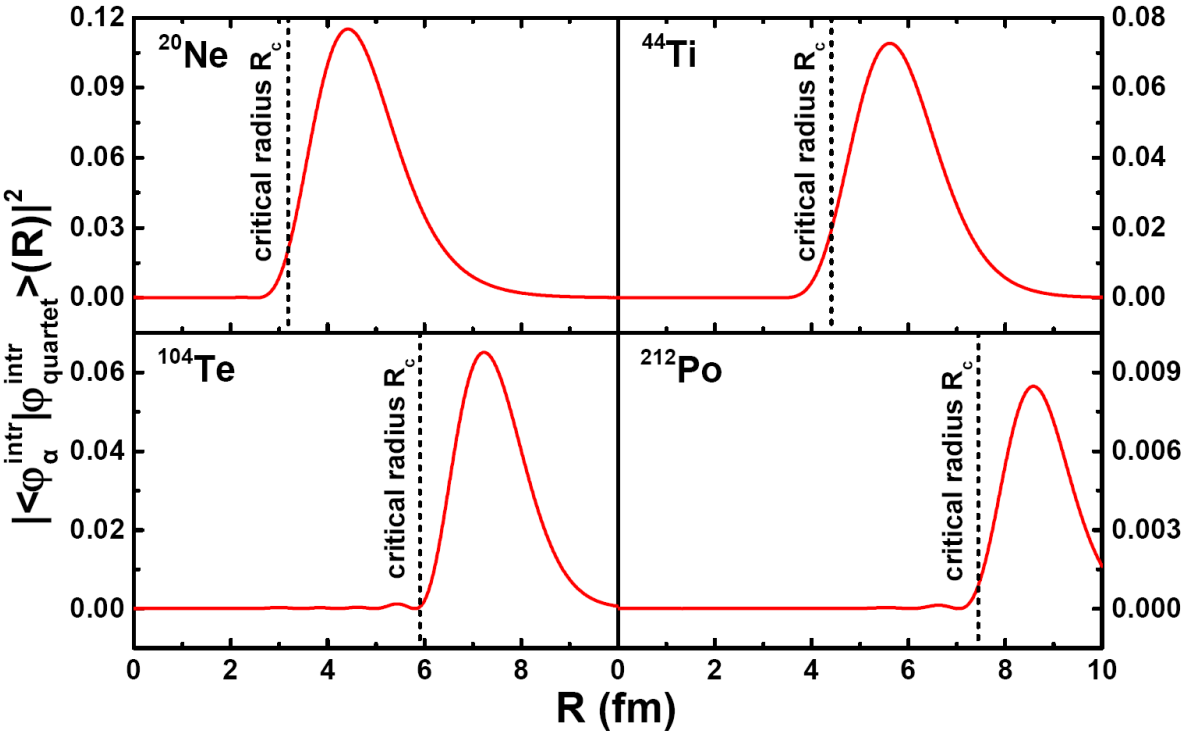

Alpha cluster formation and decay

——*Quartetting wave function approach*

First-principle approach to nuclear many-body system: several approximations performed to make the approach practicable

$$\left[-\frac{\hbar^2}{8m}\frac{\partial^2}{\partial \mathbf{R}^2}+W(\mathbf{R})\right]\Phi(\mathbf{R})=E_4\Phi(\mathbf{R}),$$

with

$$W(\mathbf{R})=E_4^{\text{intr}}(\mathbf{R})=W^{\text{ext}}(\mathbf{R})+W^{\text{intr}}(\mathbf{R})$$
$$=W^{\text{ext}}(\mathbf{R})+E_\alpha^{(0)}+W^{\text{Pauli}}(\mathbf{R})$$

$$-\frac{\hbar^2}{4m}\int d^9s_j\varphi^{\text{intr},*}(\mathbf{s}_j,\mathbf{R})[\nabla_R\varphi^{\text{intr}}(\mathbf{s}_j,\mathbf{R})]$$
$$\times[\nabla_R\Psi^{\text{com}}(\mathbf{R})]$$
$$-\frac{\hbar^2}{8m}\int d^9s_j\varphi^{\text{intr},*}(\mathbf{s}_j,\mathbf{R})\left[\nabla_R^2\varphi^{\text{intr}}(\mathbf{s}_j,\mathbf{R})\right]\Psi^{\text{com}}(\mathbf{R})$$

equation for the c.m. motion

The interaction of the quartet with core contains not only the direct NN interaction but also exchange term/Pauli-blocking

$$W^{\text{Pauli}}(n_B)\approx 4515.9\,\text{MeV fm}^3 n_B-100935\,\text{MeV fm}^6 n_B^2+1202538\,\text{MeV fm}^9 n_B^3$$

Alpha cluster formation and decay

——*Quartetting wave function approach*

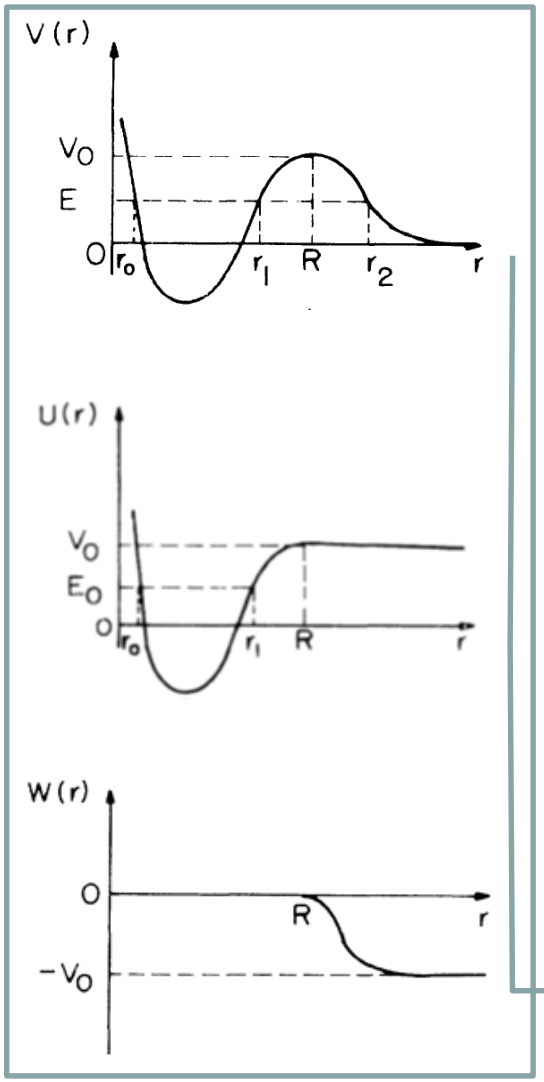

Inside the core the intrinsic W.F. describes 4 independent nucleons in quasiparticle states, whereas it changes character if a bound state is formed on the surface region, and becomes alpha-like

$$P_\alpha = \int_0^\infty d^3r |\Phi(r)|^2 \Theta\left[n_B^{\text{Mott}} - n_B(r)\right]$$

Decay width self-consistently obtained by solving both the c.o.m. motion equation of the quartet and the scattering state of the formed alpha-cluster

$$\Gamma = \nu \times \mathcal{T} = \frac{4\hbar^2\alpha^2}{\mu k} |\Phi(r_{\text{sep}})\chi_k(r_{\text{sep}})|^2$$

PHYSICAL REVIEW C VOLUME 42, NUMBER 2 AUGUST 1990

Systematics of alpha decay half-lives

Yuichi Hatsukawa
Department of Radioisotopes, Japan Atomic Energy Research Institute, Tokai, Ibaraki 319-11, Japan

Hiromichi Nakahara
Department of Chemistry, Tokyo Metropolitan University, Setagaya, Tokyo 158, Japan

Darleane C. Hoffman
Lawrence Berkeley Laboratory, University of California, Berkeley, California 94720

T_{cal}/T_{exp}

alpha cluster preformation systematics

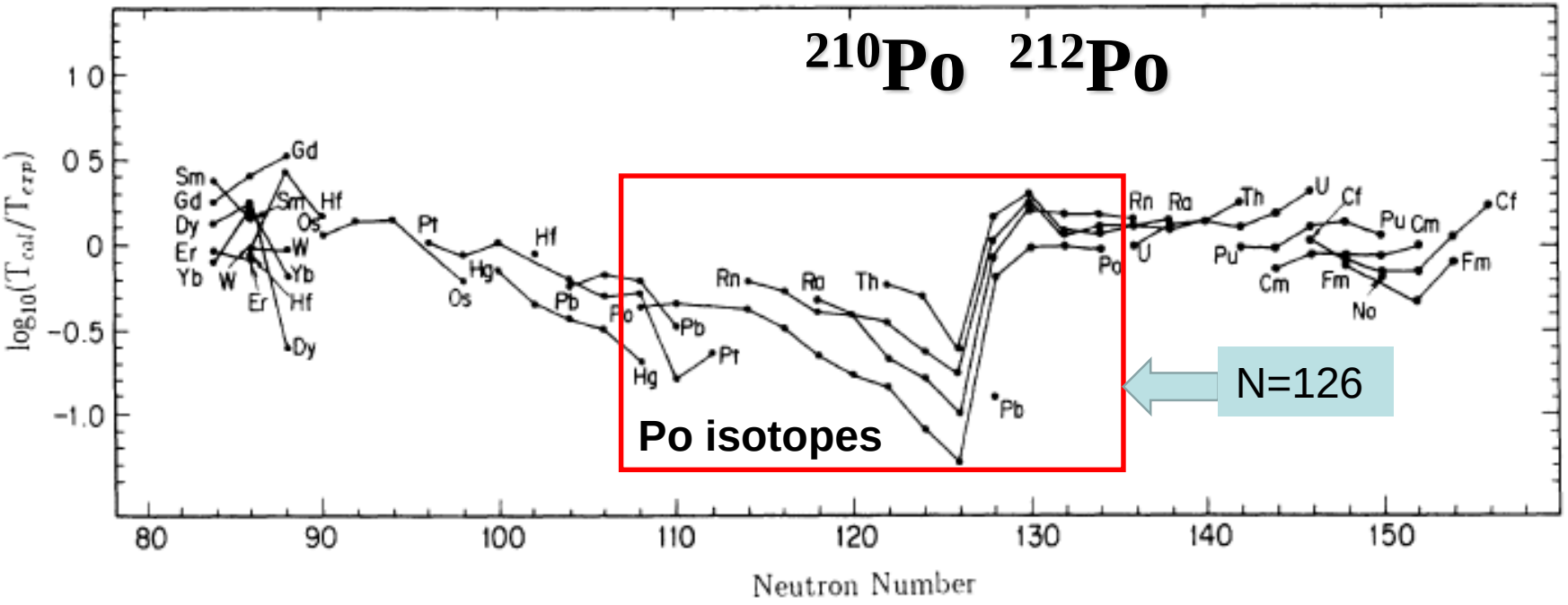

Alpha decay in ^{104}Te, ^{210}Pb, ^{210}Po, and ^{212}Po

Parent	Z	N	Q_α [MeV]	P_α	$T_{1/2}^{\text{calc.}}$ [s]	$T_{1/2}^{\text{expt.}}$ [s]
^{102}Sn	50	52		0.0551		
^{102}Te	52	50		0.3718		
^{104}Te	52	52	4.900	0.7235	1.479×10^{-8}	$<1.8\times10^{-8}$
^{210}Pb	82	128	3.792	0.0176	1.777×10^{16}	3.701×10^{16}
^{210}Po	84	126	5.408	0.0137	1.060×10^{7}	1.196×10^{7}
^{212}Po	84	128	8.954	0.1045	3.395×10^{-7}	2.997×10^{-7}

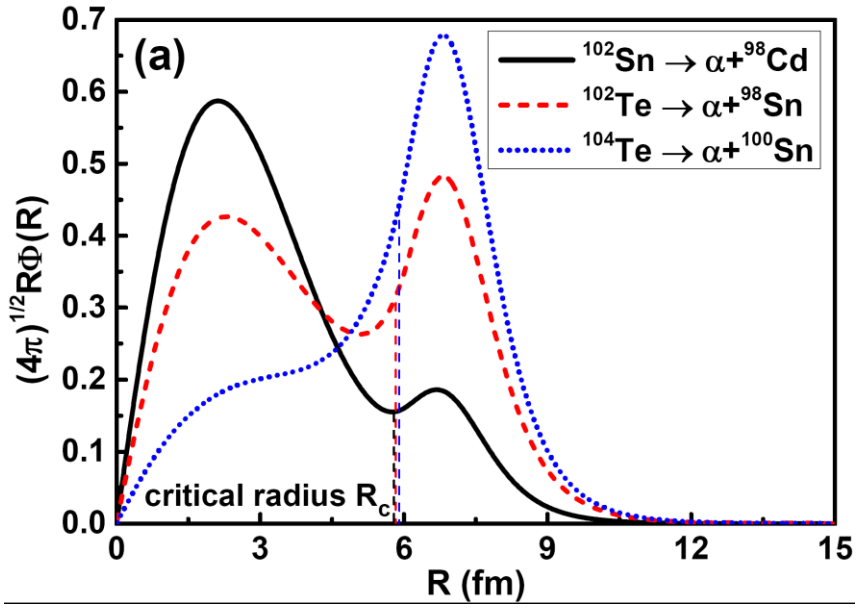

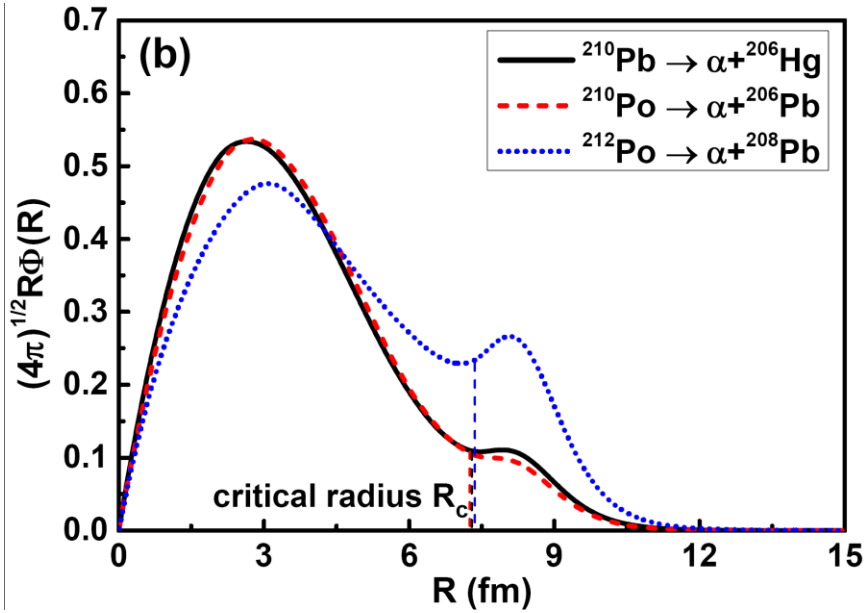

^{208}Pb: Neutron skin thickness and symmetry energy

PHYSICAL REVIEW LETTERS **126,** 172502 (2021)

Editors' Suggestion | Featured in Physics

Accurate Determination of the Neutron Skin Thickness of ^{208}Pb through Parity-Violation in Electron Scattering

^{208}Pb

We report a precision measurement of the parity-violating asymmetry A_{PV} in the elastic scattering of longitudinally polarized electrons from ^{208}Pb. We measure $A_{PV} = 550 \pm 16(\text{stat}) \pm 8(\text{syst})$ parts per billion, leading to an extraction of the neutral weak form factor $F_W(Q^2 = 0.00616\ \text{GeV}^2) = 0.368 \pm 0.013$. Combined with our previous measurement, the extracted neutron skin thickness is $R_n - R_p = 0.283 \pm 0.071$ fm. The result also yields the first significant direct measurement of the interior weak density of ^{208}Pb: $\rho_W^0 = -0.0796 \pm 0.0036(\text{exp}) \pm 0.0013(\text{theo})\ \text{fm}^{-3}$ leading to the interior baryon density $\rho_b^0 = 0.1480 \pm 0.0036(\text{exp}) \pm 0.0013(\text{theo})\ \text{fm}^{-3}$. The measurement accurately constrains the density dependence of the symmetry energy of nuclear matter near saturation density, with implications for the size and composition of neutron stars.

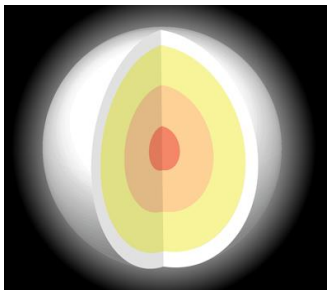

PREX: Thick skin in ^{208}Pb: stiff symmetry energy and large L

PHYSICAL REVIEW LETTERS **129,** 042501 (2022)

Editors' Suggestion

Precision Determination of the Neutral Weak Form Factor of ^{48}Ca

^{48}Ca

We report a precise measurement of the parity-violating (PV) asymmetry A_{PV} in the elastic scattering of longitudinally polarized electrons from ^{48}Ca. We measure $A_{PV} = 2668 \pm 106(\text{stat}) \pm 40(\text{syst})$ parts per billion, leading to an extraction of the neutral weak form factor $F_W(q = 0.8733\ \text{fm}^{-1}) = 0.1304 \pm 0.0052(\text{stat}) \pm 0.0020(\text{syst})$ and the charge minus the weak form factor $F_{ch} - F_W = 0.0277 \pm 0.0055$. The resulting neutron skin thickness $R_n - R_p = 0.121 \pm 0.026(\text{exp}) \pm 0.024(\text{model})$ fm is relatively thin yet consistent with many model calculations. The combined CREX and PREX results will have implications for future energy density functional calculations and on the density dependence of the symmetry energy of nuclear matter.

CREX: Thin skin in ^{48}Ca: soft symmetry energy and small L

L values deduced from PREX-2 and CREX experiments: NOT consistent with each other

Special attention has been devoted to the problem of α-clustering at the surface of nuclei that is expected to affect L value

Key quantity: **Cluster formation probability**

Key effect: **shell structure effect**

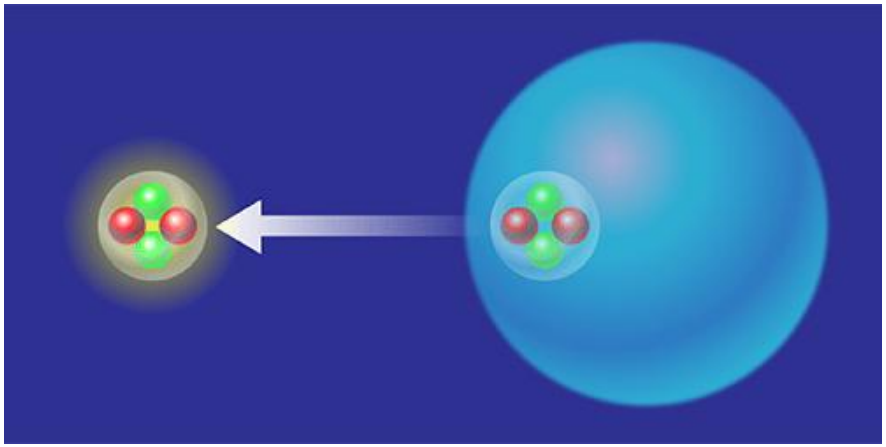

S. Typel, *Phys. Rev. C* 89, 064321 (2014)
R. Essick , *Phys. Rev. Lett.* 127, 192701 (2021)

Impact of alpha clustering on nuclear symmetry energy

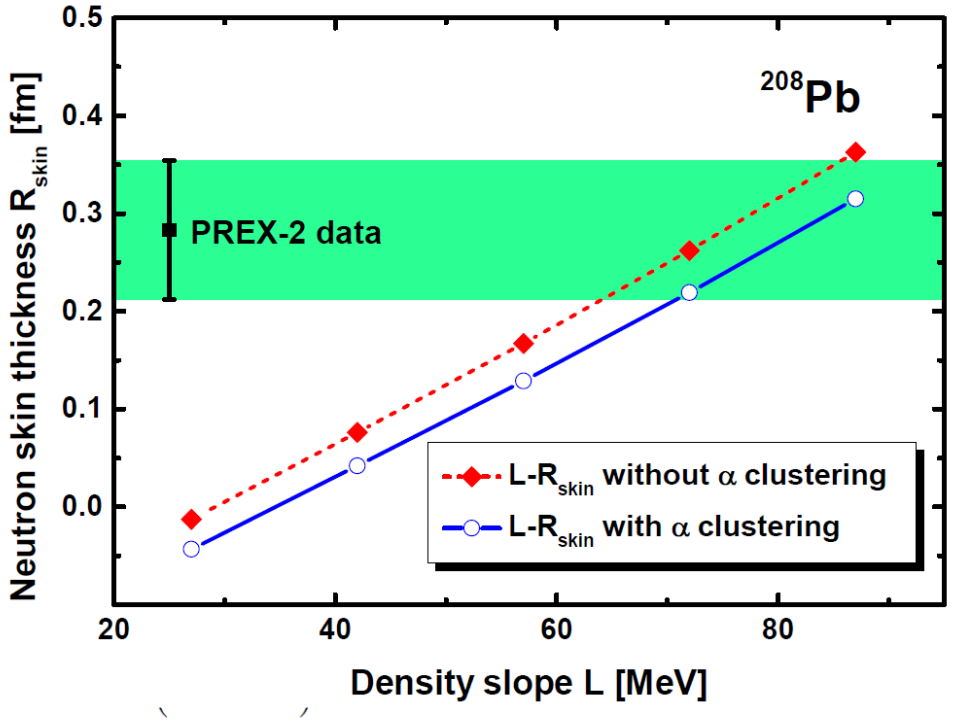

L values deduced from PREX-2 and CREX experiments are NOT consistent with each other, even with alpha clustering

75 MeV vs 16.5 MeV

Nuclei	$R_{\rm skin}$ [fm]	L [MeV] no α-cluster	P_α	L [MeV] with α-cluster
^{208}Pb	0.283±0.071	$74.9^{+24.6}_{-24.2}$	7.7×10^{-3}	$75.0^{+24.6}_{-24.2}$
^{48}Ca	0.121±0.050	$13.2^{+25.5}_{-25.1}$	0.126	$16.5^{+25.6}_{-25.2}$
*	0.071 (lower)	2.5	0.126	4.7
*	0.171 (upper)	24.9	0.126	28.3

*The correction of L due to α-clustering for the lower and upper limits of $R_{\rm skin}$ is 14% and 88%, respectively.

PREX-2: unaffected

CREX: significant

α cluster + deformed doubly magic core ^{270}Hs

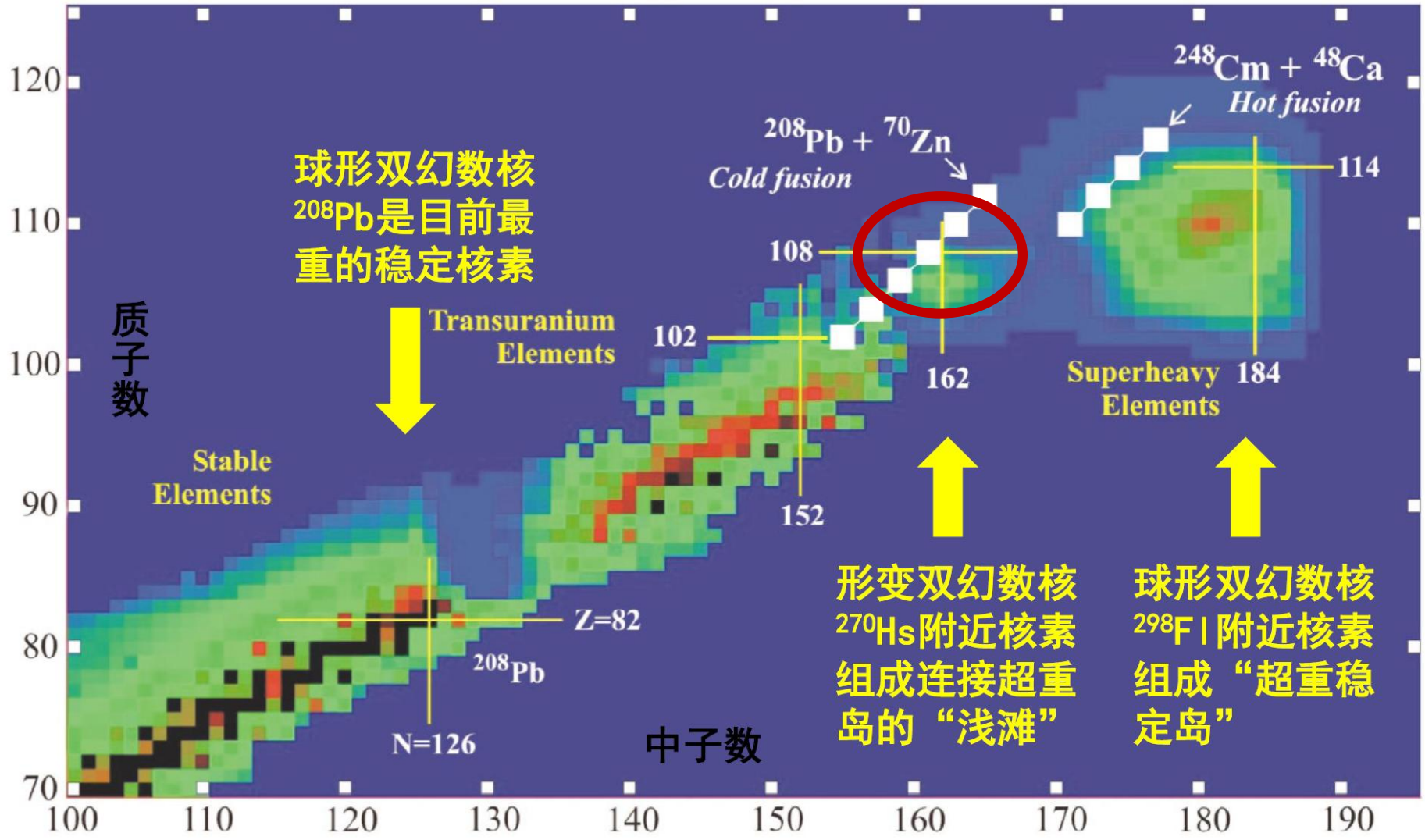

α cluster + deformed doubly magic core ^{270}Hs

Featured in Physics

Doubly Magic Nucleus $^{270}_{108}Hs_{162}$

J. Dvorak, W. Brüchle, M. Chelnokov, R. Dressler, Ch. E. Düllmann, K. Eberhardt, V. Gorshkov, E. Jäger, R. Krücken, A. Kuznetsov, Y. Nagame, F. Nebel, Z. Novackova, Z. Qin, M. Schädel, B. Schausten, E. Schimpf, A. Semchenkov, P. Thörle, A. Türler, M. Wegrzecki, B. Wierczinski, A. Yakushev, and A. Yeremin

Phys. Rev. Lett. **97**, 242501 – Published 14 December 2006

Physics See Focus story: A Nuclear Magic Trick

286	114	172	10.370	3.5×10^{-1}	17237.40	4892.79	-18.349	-17.930	0.419	0.104
270	**110**	**160**	11.117	2.1×10^{-4}	17079.10	4847.45	-17.547	-17.183	**0.364**	**0.144**
268	**108**	**160**	9.623	1.4×10^{0}	15653.10	4516.39	-19.171	-18.677	**0.494**	**0.077**
264	108	156	10.591	1.1×10^{-3}	17054.60	4843.76	-18.088	-17.709	0.379	0.140
260	106	154	9.901	1.2×10^{-2}	17488.80	4948.93	-18.759	-18.399	0.360	0.152

α cluster + deformed doubly magic core ^{270}Hs

Three-dimensional approach applied to quasistationary states of deformed *α* emitters

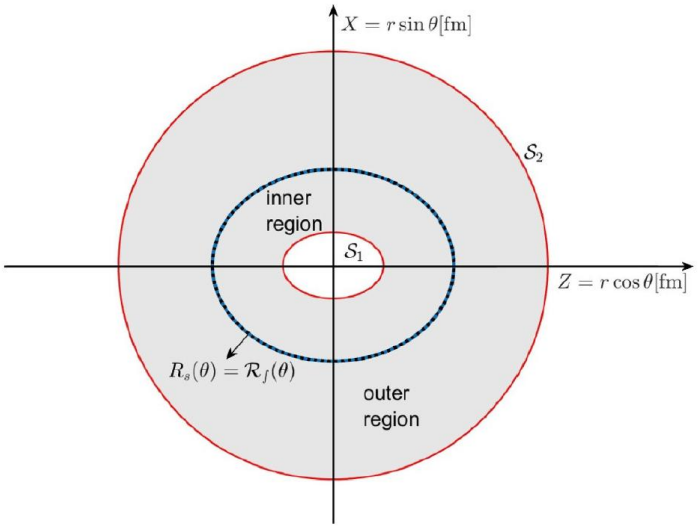

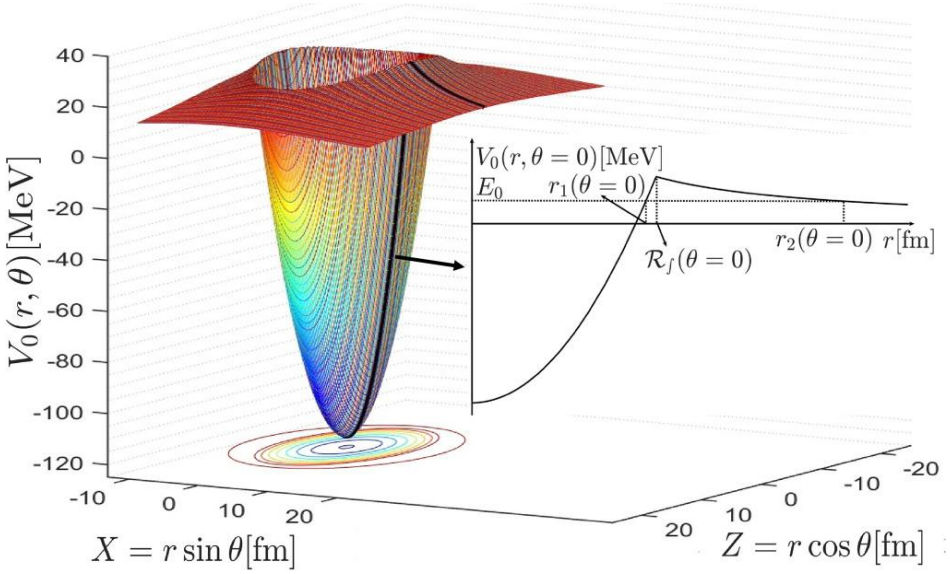

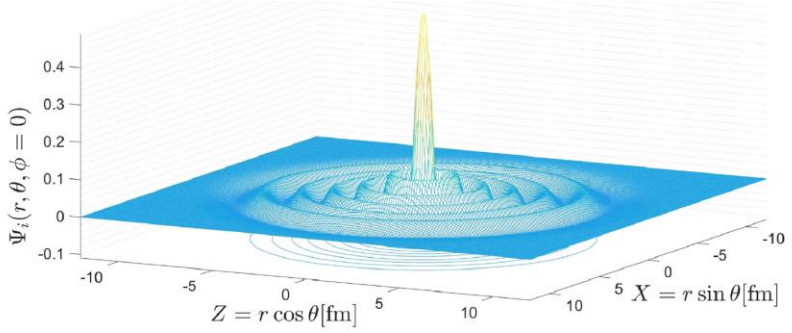

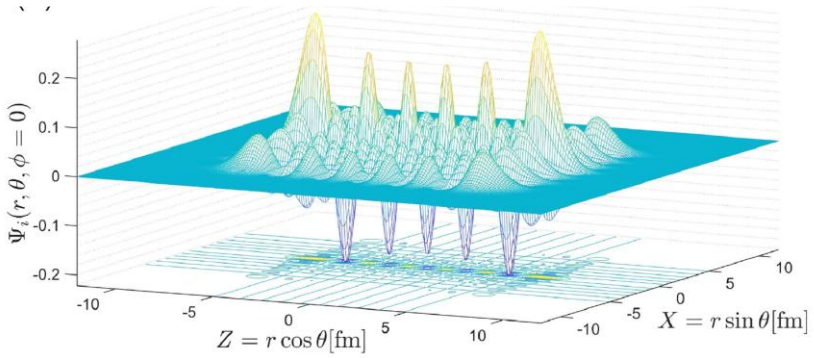

PHYSICAL REVIEW C **107**, 064301 (2023)

α cluster + deformed doubly magic core ^{270}Hs

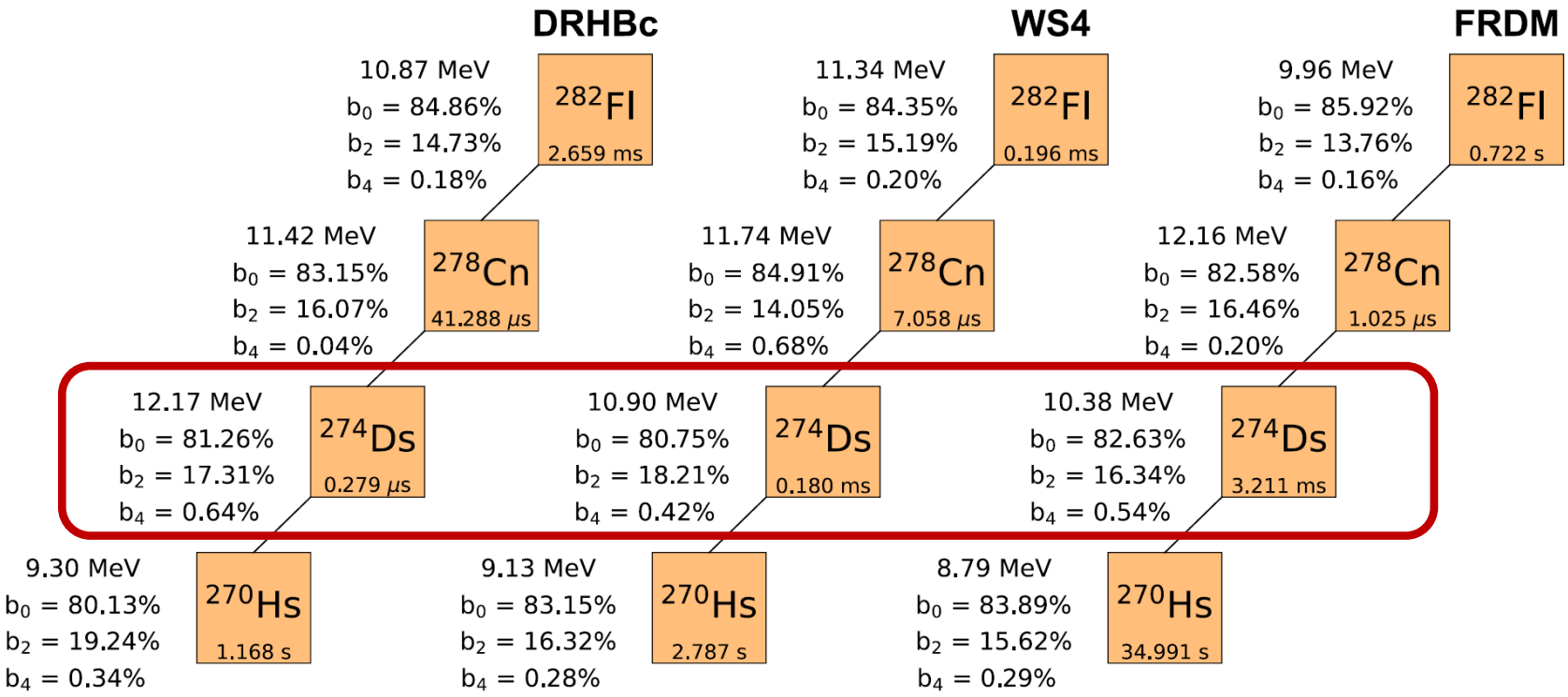

For transitions between ground states the decay energy is
α decay Q value = B(α) - [B(Z,N) - B(Z-2,N-2)]

PHYSICAL REVIEW C **110**, 054317 (2024)

Superheavy elements

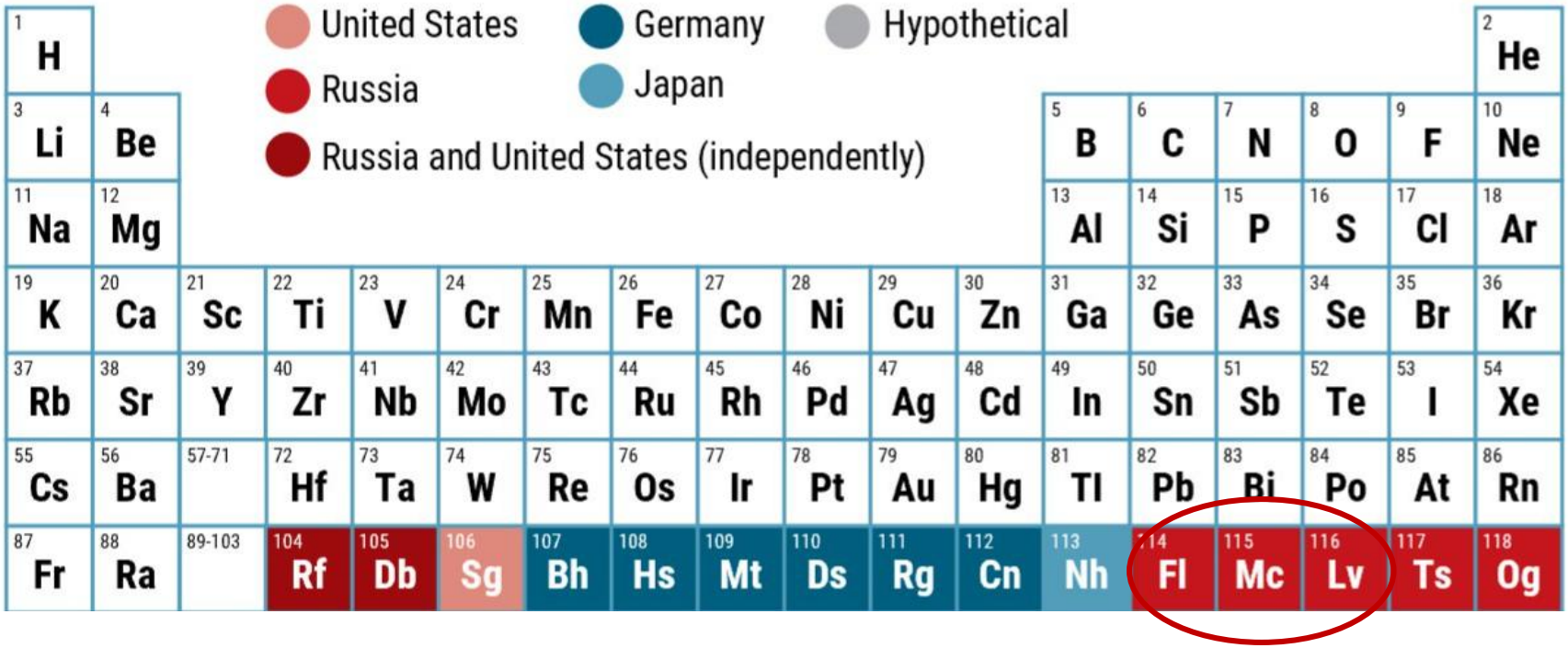

Preliminary results have been obtained by combining the predictions of modern mass model and QWFA

$^{302}Lv \rightarrow {}^{298}Fl + \alpha$ (?) ***Z=114; N=184***

Nuclear Physics Across Energy Scales conference, C3NT, Wuhan

- ***A strict microscopic model based on a first-principle approach to nuclear many-body systems***
- ***Alpha-cluster formation and dissolution in nuclei are correctly described by solving quantum four-body equations in nuclear medium***
- ***Pauli blockings and shell structure effects on alpha-clustering and decay are accounted for in QWFA***

Thanks for your attention

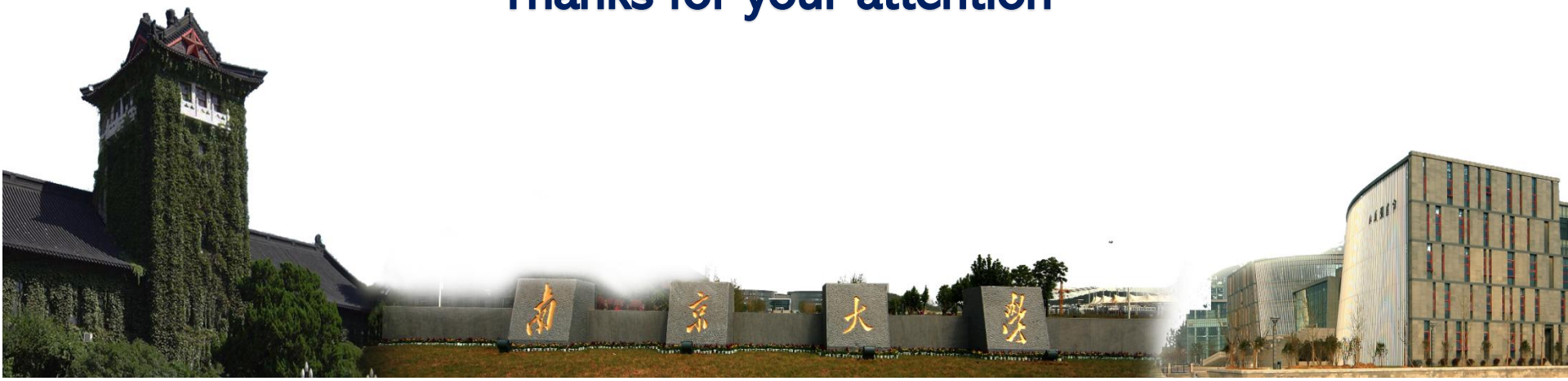

Nuclear symmetry energy and its density slope

symmetry energy

Isospin asymmetry

$$E(\rho_n,\rho_p) = E_0(\rho_n = \rho_p) + E_{sym}(\rho)\left(\frac{\rho_n - \rho_p}{\rho}\right)^2 + o(\delta^4)$$

Energy per nucleon in symmetric nuclear matter

Energy per nucleon in asymmetric nuclear matter

The symmetry energy can be characterized by the $E_{\rm sym}(\rho_0)$ and its slope parameter $L(\rho_0)$

$$E_{\rm sym}(\rho) = E_{\rm sym}(\rho_0) + \frac{L(\rho_0)}{3}\left(\frac{\rho-\rho_0}{\rho_0}\right) + O\left[\left(\frac{\rho-\rho_0}{\rho_0}\right)^2\right]$$

$$L(\rho_0) = 3\rho\frac{\partial E_{\rm sym}(\rho)}{\partial\rho}\bigg|_{\rho=\rho_0}$$

Derivative of density

Derivative of momentum at normal density

PHYSICAL REVIEW C
covering nuclear physics

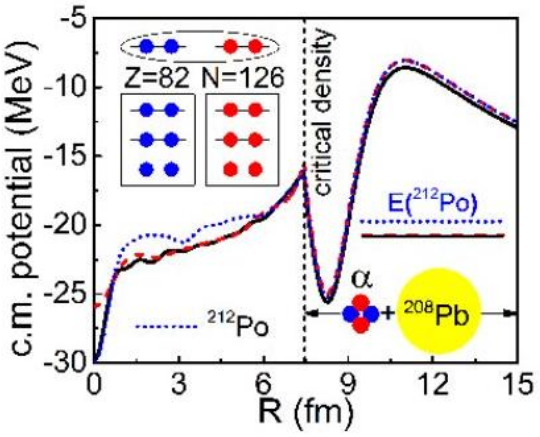

EDITORS' SUGGESTION

α decay to a doubly magic core in the quartetting wave function approach

This microscopic calculation for the α decay of heavy nuclei provides a solution to what has long been an outstanding problem. In the authors' model, the α particle exists only below about one-fifth of saturation density, corresponding to a large radius, inside of which the α particle transitions into an unbound four-nucleon shell-model state. The model reproduces the half-life of ^{212}Po (a classic test case) as well as some neighboring nuclei, and calculations are also made for ^{104}Te.

***Phy. Rev. Editor* "This microscopic calculation for the alpha decay of heavy nuclei provides a solution to what has long been an outstanding problem"**

Alpha cluster formation and decay

——*Quartetting wave function approach*

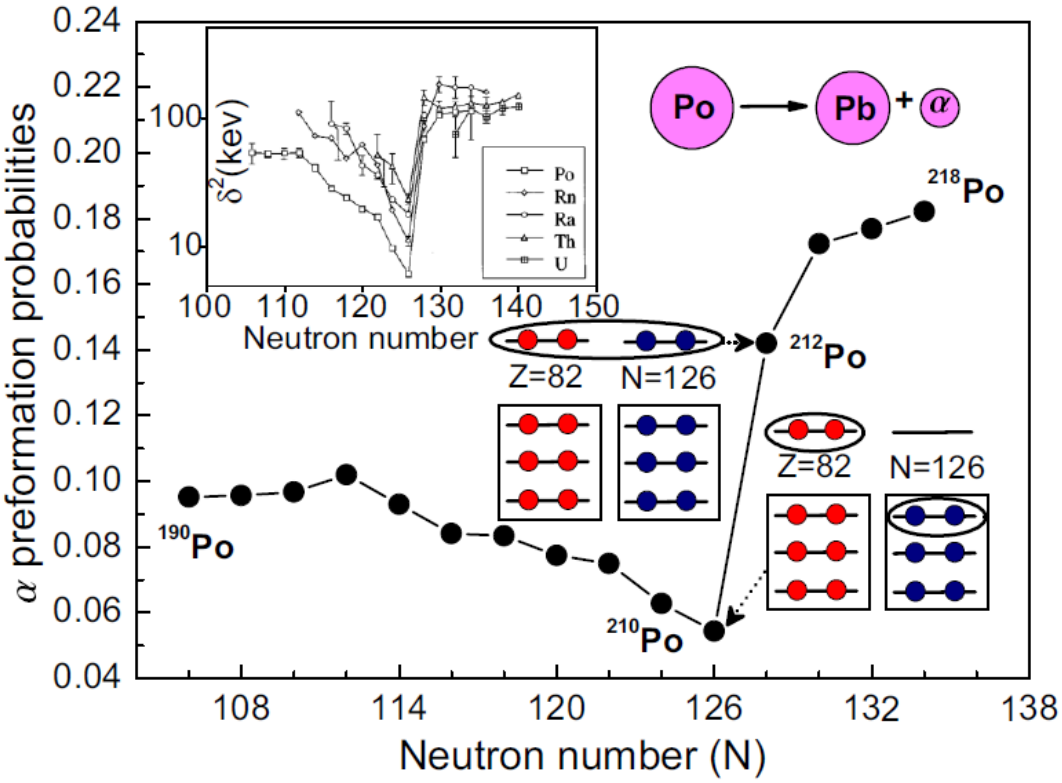

Experimental data:
Qa and Ta (well measured)

c and *d* fitted to Qa and Ta

Preformation probabilities are obtained for each nucleus

shell effect: further improments

$$v(s) = c\exp(-4s)/(4s) - d\exp(-2.5s)/(2.5s)$$

describing a short-range repulsion (*c*) and a long-range attraction (*d*);
S denotes the nucleon-nucleon distance.

Using the Hugenholtz–Van Hove (HVH) theorem

$$t(k_F^n) + U_n(\rho,\delta,k_F^n) = \frac{\partial \xi}{\partial \rho_n},$$
$$t(k_F^p) + U_p(\rho,\delta,k_F^p) = \frac{\partial \xi}{\partial \rho_p},$$

$$U_\tau(\rho,\delta,k) = U_0(\rho,k) + \sum_{i=1,2,3,\ldots} U_{\mathrm{sym},i}(\rho,k)(\tau\delta)^i$$
$$= U_0(\rho,k) + U_{\mathrm{sym},1}(\rho,k)(\tau\delta) + U_{\mathrm{sym},2}(k)(\tau\delta)^2 + \cdots$$

Left side

$$[t(k_F^n) - t(k_F^p)] + [U_n(\rho,\delta,k_F^n) - U_p(\rho,\delta,k_F^p)]$$
$$= \sum_{i=1,2,3,\ldots} \frac{1}{i!} \frac{\partial^i [t(k) + U_0(\rho,k)]}{\partial k^i}\bigg|_{k_F} k_F^i$$
$$\times \left[\left(\sum_{j=1,2,3,\ldots} F(j)\delta^j \right)^i - \left(\sum_{j=1,2,3,\ldots} F(j)(-\delta)^j \right)^i \right]$$
$$+ \sum_{l=1,2,3,\ldots} U_{\mathrm{sym},l}(\rho,k_F)[\delta^l - (-\delta)^l] + \sum_{l=1,2,3,\ldots} \sum_{i=1,2,3,\ldots} \frac{1}{i!} \frac{\partial^i U_{\mathrm{sym},l}(\rho,k)}{\partial k^i}\bigg|_{k_F} k_F^i$$
$$\times \left[\left(\sum_{j=1,2,3,\ldots} F(j)\delta^j \right)^i \delta^l - \left(\sum_{j=1,2,3,\ldots} F(j)(-\delta)^j \right)^i (-\delta)^l \right]$$
$$= \left[\frac{2}{3} \frac{\partial [t(k) + U_0(\rho,k)]}{\partial k}\bigg|_{k_F} k_F + 2U_{\mathrm{sym},1}(\rho,k_F) \right] \delta + \cdots,$$

Right side

$$\frac{\partial \xi}{\partial \rho_n} - \frac{\partial \xi}{\partial \rho_p} = \frac{2}{\rho}\frac{\partial \xi}{\partial \delta} = \sum_{i=2,4,6,\ldots} 2i\, E_{\mathrm{sym},i}(\rho)\delta^{i-1}$$
$$= 4E_{\mathrm{sym},2}(\rho)\delta + 8E_{\mathrm{sym},4}(\rho)\delta^3 + 12E_{\mathrm{sym},6}(\rho)\delta^5 + \cdots$$

Isoscalar and isovector potentials: U_0 and U_{sym}

Symmetry energy of any order: E_{sym}

Analytical formula: symmetry energy and density slope

$$E_{\rm sym}(\rho_0) = \frac{1}{6}\left.\frac{\partial(t+U_0)}{\partial k}\right|_{k_F} k_F + \frac{1}{2}U_{\rm sym}(\rho_0,k_F)$$

$$= \frac{1}{3}t(k_F) + \frac{1}{6}\left.\frac{\partial U_0}{\partial k}\right|_{k_F} k_F + \frac{1}{2}U_{\rm sym}(\rho_0,k_F)$$

isoscalar

$$L(\rho_0) = \frac{1}{6}\left.\frac{\partial(t+U_0)}{\partial k}\right|_{k_F} k_F + \frac{1}{6}\left.\frac{\partial^2(t+U_0)}{\partial k^2}\right|_{k_F} k_F^2 + \frac{3}{2}U_{\rm sym}(\rho_0,k_F) + \left.\frac{\partial U_{\rm sym}(\rho_0,k)}{\partial k}\right|_{k_F} k_F$$

isovector

Lane potential

Derivative of momentum at normal density

Xu et. al, *PRC* 81, 044603 (2010); *NPA* 865, 1 (2011); *PRC* 90, 064310 (2014)